Universidade de Évora - Escola de Ciências e Tecnologia Universidade de Lisboa - Instituto Superior de Agronomia

Mestrado em Gestão e Conservação de Recursos Naturais

Dissertação

Megafauna large-scale distribution patterns along the Gloria Fracture Zone (NE Atlantic)

Teresa Regina Cardoso Ferreira

Orientador(es) | Helena Adão

Sofia Alexandra Pinto Ramalho

Évora 2022

Universidade de Évora - Escola de Ciências e Tecnologia Universidade de Lisboa - Instituto Superior de Agronomia

Mestrado em Gestão e Conservação de Recursos Naturais

Dissertação

Megafauna large-scale distribution patterns along the Gloria Fracture Zone (NE Atlantic)

Teresa Regina Cardoso Ferreira

Orientador(es) | Helena Adão

Sofia Alexandra Pinto Ramalho

Évora 2022

A dissertação foi objeto de apreciação e discussão pública pelo seguinte júri nomeado pelo Diretor da Escola de Ciências e Tecnologia:

Presidente	|	Pedro R. Almeida (Universidade de Évora)
Vogais	|	Clara Lúcia Ferreira Rodrigues (Universidade de Aveiro) (Arguente) Sofia Alexandra Pinto Ramalho (Universidade de Aveiro) (Orientado

Évora 2022

ACKNOWLEDGEMENTS

First and foremost, I would like to thank my supervisors Helena Adão and Sofia Ramalho for allowing me to work on such an exciting theme. I would like to thank them for the highly valued advice and moral support throughout the development of this thesis and I am hopeful my work reflects their dedication in guiding me and making sure no doubts were left behind. A special thanks to Sofia for the constant availability, patience and thorough attention in pointing out what needed improvement in my work, which encouraged me to always do better, but also for guiding me to other amazing opportunities, namely experiencing life out at sea.

In addition, the work of this thesis would have not been possible without the data collected on board of the R/V Meteor during the Flows expedition (M162) in March 2019, so I would like to extend my thanks to everyone who had a role in collecting all the data and imagery used.

Finally, it would have been hard to go through this experience without the unconditional care of my mum and boyfriend, so I would like to thank them for always being present and for the kind reminders of my strengths, when I felt overwhelmed by my weaknesses.

RESUMO

Padrões de distribuição de megafauna a grande escala ao longo da zona da falha Gloria (Atlântico NE)

As falhas cobrem extensas áreas de fundos marinhos e estão associadas a paisagens e contextos ambientais complexos. Neste estudo foram utilizadas imagens capturadas em quatro áreas para caracterizar a mega-epifauna bentónica ao longo da falha Gloria e os resultados foram explorados considerando a variação ambiental. As variáveis ambientais investigadas revelaram similaridade entre o segmento ocidental e central. Nestas áreas, as densidades de mega-epifauna foram menores, mas a composição variou devido a diferenças entre proporções de Anthozoa e Holothuroidea. Pelo contrário, no segmento oriental foram observadas as maiores densidades e maiores proporções de Anthozoa. O rift da Terceira apresentou uma das maiores densidades e constituiu uma das áreas mais diversas, possivelmente devido á maior produtividade e variedade de substrato observada. Este estudo apresenta pela primeira vez resultados referentes aos padrões de distribuição e diversidade de fauna abissal ao longo da falha Gloria, com relevância para a futura gestão e conservação, inclusivamente de áreas de jurisdição nacional.

ABSTRACT

Megafauna large-scale distribution patterns along the Gloria Fracture Zone (NE Atlantic)

Faults are extensive seafloor features associated with large-scale landscape and environmental complexity. This study focused on the characterization of benthic mega-epifaunal assemblages explored in relation to environmental setting, using imagery surveys carried along four areas of the Gloria Fault. The environmental variables investigated revealed similarity between western and central segments of the Gloria Fault. In these two areas lower densities were observed, but composition showed variability, due to different proportions of Anthozoa and Holothuroidea. By opposition, the highest total density was observed at the eastern segment, where high proportions of Anthozoa were observed. The Terceira rift area was characterised by high densities and high diversity, possibly associated to higher productivity and a more diverse substrata composition. This study reports for the first-time on the spatial distribution patterns and diversity of abyssal fauna of the Gloria Fault, including in areas under national jurisdiction, with relevance for future management and conservation actions.

Table of contents

List of tables

List of figures

1. INTRODUCTION

1.1. Deep sea knowledge, exploration gap and current threats

Oceans cover approximately 70% of earth's surface and about 50% of it, is designated as deep sea (c.a. >200m water depth) (Ramirez-Llodra et al., 2011). The deep sea is therefore considered the largest ecosystem on earth and a biodiversity hotspot (Ramirez-Llodra et al., 2010). It provides essential ecosystem functions and services, such as nutrient cycling and carbon sequestration and plays an essential role in climate regulation (Armstrong et al., 2012; Thurber et al., 2014). However, its remoteness among other factors, make it difficult to survey, still limiting today our understanding of this unique environment (Ramirez-Llodra et al., 2010).

For a long time, the deep sea was regarded as lifeless (Forbes, 1844), even though in the late 18th several specimens had been collected by fishermen from depths greater than 200 m and described by naturalists (Etter and Hess, 2015). Faulty perceptions about the deep sea were only contradicted after several expeditions were undertaken around the globe, providing solid evidence that life prevailed at great depths (Tyler et al., 2003). Yet, it was only in the last few decades that technological advancements have allowed to capture a wider range of deep-sea habitats, diversity of processes and organisms (Gage, 1996; Clark et al., 2016a). For instance, it was only 44 years ago that hydrothermal vents were first discovered at the Galapagos Rift in the Pacific, overflowing with undiscovered organisms, dependent on chemosynthesis to survive (Lonsdale et al., 1977). Today, access to complex and highly technical instrumentations allows us, among other things, to photograph species and communities *in situ*, observe behaviour of deep-sea organisms, and even perform *in-situ* experimental works, while avoiding damaging habitats or organisms (Clark et al., 2016a). Nevertheless, it is important to recognise that we still have an extremely poor spatial and temporal resolution of deep-sea observations, with approximately 20.6% of the world ocean's floor mapped with multi-beam echo sounding technology and very small portion either sampled or remotely surveyed (Ramirez-Llodra et al., 2010; Seabed 2030 Project, 2021).

Even though our knowledge about this remote environment is scarce, most regions are already impacted by one or multiple sources of human induced pressure, arising either from natural resource exploitation, pollution and waste disposal, or alterations associated with climate change (Ramirez-Llodra et al., 2011). For instance, bottom trawling fisheries, known to induce irreversible changes in diverse habitats, represent one the most widespread forms of resource exploitation (Clark et al., 2016b). Another example is pollution by marine litter. Despite the fact that higher quantities are typically observed near coastal areas, marine litter presents a widespread occurrence and is already found in the deepest parts of our oceans (Pham et al., 2014; Chiba et al., 2018).

The limited understanding of our oceans, particularly at great depths, has led to the creation of the UN Decade of Ocean Science for Sustainable Development programme (2021-2030), including deep-sea-focused Ocean Decade Actions (Howell et al., 2020a, 2020b). This program has established priority target areas and habitats and provided methodological guidelines that are intended to allow coherent integration of data, as well as support the establishment of informed monitoring and conservation actions for deep-sea regions (Howell et al., 2020a, 2020b).

1.2. Life in the deep sea

The deep sea starts topographically at the continental shelf break where the light becomes limited (typically around 200 m water depth) and extends down to the deepest point of our oceans (around 11 000 m water depth) (Tyler, 2003). The deep seafloor can be divided into three major zones, the bathyal (200-3000 m), abyssal (3000-6000 m) and hadal zone (6000-11000 m) (Tyler, 2003; Ramirez-Llodra et al., 2010). Within these zones, a wide variety of seafloor habitats can be found, including important geological formations, such as submarine canyons, seamounts, seeps, hydrothermal vents, but also extremely large habitats, such as abyssal plains, trenches and mid-ocean ridges (Ramirez-Llodra et al., 2010).

Deep-sea habitats are characterised by absence of light, generally high-pressure conditions (rises 1 atm per every 10 m), low yet stable temperatures (c.a., 2 – 4 ºC), high oxygen concentrations (5-6 $ml.l^{-1}$) and constant salinity levels (Tyler, 2003). Particularly important to the organisms that live in these areas is the shortage of food availability (Tyler, 2003; Smith et al., 2008). The organic matter that reaches the bottom is essentially in the form the particulate organic carbon (POC) derived primarily from production occurring in the euphotic zone, that has travelled through the water column and decomposed (Ramirez-Llodra et al., 2010). The faunal dependency on heterotrophic food sources is only disrupted where *in-situ* chemosynthetic production occurs, for example at hydrothermal vents, cold seeps, or organic falls sites, namely in the form of whale carcases or wood falls (e.g., Smith and Baco, 2003; Åström et al.,2018). In these locations, organic matter is predominantly derived from microbial activity using energy withdrawn from the oxidation of inorganic compounds, such as hydrogen sulphide or methane (Ramirez-Llodra et al., 2010).

Evolutionary and ecological processes have been responsible for distinguishing communities inhabiting deep-sea habitats, from those of shallower waters, both in terms of their taxonomic and functional identity (Ramirez-Llodra et al., 2010). In order to survive and thrive in the deep sea, many faunal organisms are known to display adaptations that allow them to survive and thrive under the complex and often adverse environmental conditions at

great depths. Among others, organisms can display phenotypical adaptations (e.g., advantageous coloration, absence of eyes), behaviour adaptations (e.g., communication through the production of light), biochemical adaptations (e.g., specialization of the enzymatic machinery and in membranes activity) and suffer alterations in body size (e.g., dwarfism, gigantism) (Tyler, 2003; Ramirez-Llodra et al., 2010).

The deep-sea benthic metazoan fauna can be distinguished into the following size classes: meiofauna (>32 µm; Pape et al., 2021), macrofauna (>250 µm; Macdonald et al., 2010) and megafauna (>few centimetres or seen in photographs at substrates surface; Tyler, 2003). These organisms can also be distinguished in relation to their position in the environment, in which often smaller size classes belong to infauna (living inside the sediments), while larger classes, such as megafauna, are typically epibenthic (living on the surface of the substrata). The benthic fauna is involved in a variety of ecosystem functions (Strong et al., 2015). Besides participating in carbon transformation across the food web, it is also directly and indirectly involved in nutrient cycling processes and habitat engineering (Strong et al., 2015). For example, sponge grounds can contribute to carbon and nitrogen cycling processes, through consumption of suspended organic particles and dissolved organic matter (Kutti et al., 2013; Maldonado et al., 2017). Another example relates to infaunal organisms (both meio- and macrofauna) which through bioturbation and bioirrigation, allow the oxygenation of sediments and transportation of organic matter to deeper layers, promoting bacterial production and consequently nutrient cycling and carbon remineralization (Meysman et al., 2006). Mega-epifauna organisms can also promote habitat heterogeneity, by constituting biological structures, which locally change current flows and biogeochemical regimes, while also providing substrate for other species to settle, find refuge or even constituting nursing grounds for certain species of fishes (Buhl-Mortensen et al., 2010).

Faunal standing-stocks (density and biomass), diversity and distribution patterns in the deep-sea heterotrophic ecosystems are often linked with both food quantity and quality (Smith et al., 2008). As the POC fluxes decrease with depth, benthic standing stocks also decrease with greater accentuation for mega- and macrofaunal organisms (Fig.1; Rex et al., 2006). Microbial communities stand aside of such patterns exhibiting a subtle change in standing stocks with depth (Rex et al., 2006).

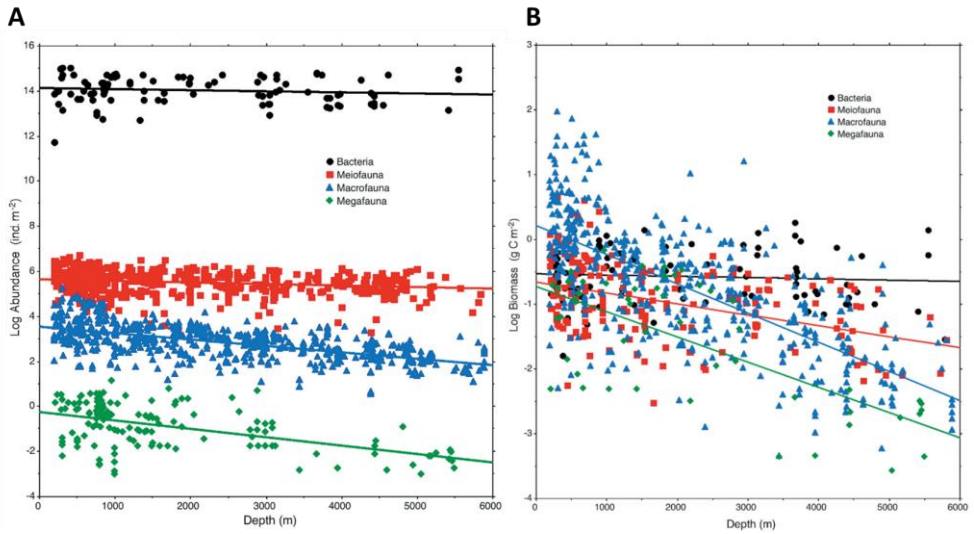

Figure 1 – (A) Abundance and **(B)** biomass as function of depth (m) for the different benthic compartments, including bacteria, meiofauna, macrofauna and mega-epifauna. From: Rex et al. (2006).

With regards to biodiversity patterns in relation to depth increases, studies have highlighted a possible unimodal pattern, where the bathyal zone potentially concentrates the highest species richness, decreasing towards shallower and greater depths (e.g., Cosson-Sarradin et al., 1998; Brandt et al., 2005; Stuart and Rex, 2009). Nevertheless, there has been indications that this pattern might not be universal across the different taxonomic groups (Smith et al., 2006; Stuart and Rex, 2009; Brandt et al., 2009). Independent of bathymetric relationships, deep-sea benthic fauna is overall considered to be diverse, with high proportion of rare species across different habitats and ocean regions (Danovaro et al., 2014; Ramirez-Llodra et al., 2010).

Noteworthy, despite the generalizations mentioned above, composition of faunal communities and associated structural and functional diversity is inevitably shaped by complex interacting ecological factors, and not just by changes in physical conditions and food supply associated with the depth gradients (Gage and Tyler, 1991).

1.3. Faunal patterns in abyssal plains

Approximately 80% of the ocean's seabed are abyssal plains, making them the vastest benthic habitats found in the deep sea (Fig.2; Harris et al., 2014). Throughout history they have been poorly studied and mistakenly perceived as homogenous and environmentally stable regions. Today, we know that these are complex and unique areas (Ebbe et al., 2010; Ramirez-Llodra et al., 2010).

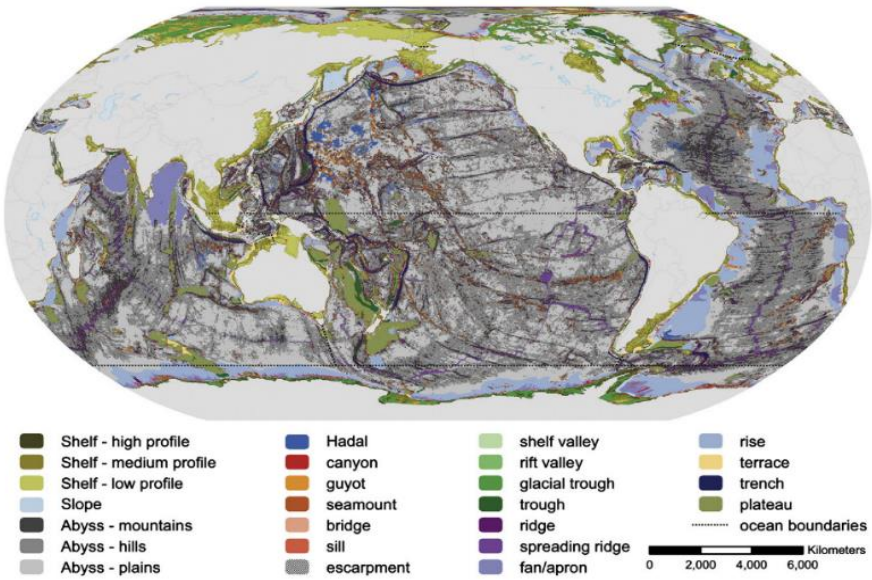

Figure 2 – Main geomorphic features of the seafloor. From: Harris et al. (2014).

Abyssal plains are defined as the seafloor areas between depths of approximately 3000 and 6000 m, generally composed by thick layers of fine sediments that can stretch through large extensions of ocean basins, interrupted by ridges, trenches or intersected by fractures zones and sometimes surrounding seamounts or guyots (Harris et al., 2014). The abyss is generally characterised by constant temperatures (-0.5 - 3.08 ºC), high oxygen supply levels (5 - 6 $ml.l^{-1}$) and constant salinity, but it is subjected to extremely high pressures and limited food supply (Smith et al., 2008; Ramirez-Llodra et al., 2010). Furthermore, abyssal areas are usually under influence of relatively slow currents (<4 $cm.s^{-1}$; Tyler et al., 2003) and tidal regimes, however, these may be disrupted by high-energy events that impose strong near-bottom currents, such as benthic storms or turbidity currents (Connolly et al. 2020).

Associated with increasing water depth and decrease in food supply, there is a general decrease in the average body-size of the benthic organisms at abyssal areas, where small size groups, such as meiofauna and macrofauna, often represent the largest proportion of the benthic fauna standing stocks (Rex et al., 2006). Nevertheless, mega-epifauna is still a key component of the abyssal benthos, promoting diversity and providing important functions, for example, at the level of organic matter transformation processes and biological engineering (Buhl-Mortesen et al., 2010).

The changes in POC flux affecting the benthos in abyssal areas are noted both in terms of depth increase and organic content degradation, but also related with distance from continental margins, where higher quantity and quality is found near coastal zones (Smith et

al., 2008). Additionally, regular or episodic disturbance events near the seafloor, such as currents and benthic storms, are known promote redistribution of particles and influence the transport organic matter across large areas (Aller, 1989; Connolly et al. 2020). Surface climate-driven events inevitably also influence food supply to the abyss (Smith et al., 2006). For example, mega-epifaunal community structure alteration has been linked to climate related changes of both El Niño and La Ninã events, evidencing that variations at surface are reflected in depth (Ruhl and Smith, 2004). Another notorious example of changes in benthic communities was recorded at the Porcupine Abyssal Plain and named as the "*Amperima event"*. In this case, a remarkable rise in density of the holothurian *Amperima rosea* was observed, possibly related to a large-scale change in POC flux to the seafloor (Billet et al., 2001; Bett et al., 2001; Billet et al., 2010;). Despite variations being firstly detected in mega-epifauna organisms, changes were also observed in Foraminifera, and on both meiofauna and macrofauna (Kalogeropoulou et al., 2009; Soto et al., 2010; Gooday et al., 2010). Furthermore, it is likely that such variations are also associated with fluctuations in ecosystem processes such as nutrient cycling and organic matter transformation (Levin et al., 2001; Smith et al., 2008).

Besides variations in food supply to the abyss, heterogenous faunal distribution patterns in abyssal areas can further arise from changes in seafloor geomorphology and inherent variations of substrates type (e.g., Durden et al., 2015; Simon-Lledó et al., 2019). Despite being particularly significant for mega-epibenthic organisms, changes in geomorphology are also likely to influence on smaller sized groups (Vanreusel et al., 2010). Although designated by "plains", the abyssal landscape is complex, interrupted for example, by elevated topographic structures such as hills (higher than 300 m and smaller 1000 m) and seamounts (higher than 1000 m), or troughs (Harris et al., 2014). Deep-water elevation structures, such as hills and seamounts, represent obstacles that diffuse or modify currents and near bottom flows, influencing processes of sediment sorting, organic matter deposition, larval dispersal, while also providing a wide range of substrata that can host different faunal assemblages (Levin et al., 2001; Durden et al., 2015; Cuvelier et al., 2020). These structures usually harbour significantly higher mega-epifaunal biomass and different trophic diversity by comparison to nearby abyssal flat areas (Durden et al., 2015), and in some cases communities in these elevations rarely share common taxa with adjacent areas (Cuvelier et al., 2020). Smaller landscape variations (few hundred meters) have been shown to significantly affect the benthic mega-epifaunal organisms (Simon-Lledó et al., 2019). Simon-Lledó et al. (2019) found that ridges harboured higher densities overall by comparison to the troughs, possibly because the elevation allows a higher availability of suspended particles transported by local currents,

sustaining higher proportions of sessile filtering fauna and more complex communities (Simon-Lledó et al., 2019).

Associated or not with topography, variation in substrate type, namely the presence of hard substrata in an otherwise sedimented dominated regions, is another key factor that shapes benthic fauna in the abyss. The abyssal seafloor is in fact predominantly composed of muddy sediments from both terrigenous (highest proportion when near continents) and marine origin (from the sinking of planktonic organisms, or hemipelagic particles; Tyler, 2003). Soft substrate composition is usually controlled by processes that operate both at a local and large scale, where changes are reflections of balances between rates of biological particle supply (e.g. production of shells) and rates of silica and calcium dissolution increasing with depth (Tyler, 2003). Turbidites deposition areas may also occur in some abyssal regions, such as the Madeira Abyssal Plain, resultant from the rapid accumulation of sediments after gravity flow events (Tyler, 2003). The presence of spare or large hard rock aggregations serves as the ultimate disruption to the assumed homogenous abyssal seafloor sediment composition (Tyler, 2003; Riehl et al., 2020). This allows the establishment of fauna that would not otherwise be present and may represent stepping-stone areas for sessile fauna, promoting connectivity across large areas in the ocean basins (Smith et al., 2006). Another notorious evidence of the significance of hard substrata in abyssal regions are the polymetallic nodules. Vanreusel et al (2016) concluded that nodule covered sites are essential to support coral communities, otherwise absent or only found in low numbers in nodule free locations (Vanreusel et al., 2016). Other examples include drop stones near polar areas (Ziegler et al., 2017) or hard substrata exposure along fracture zones (Riehl et al., 2020). Similarly, these prove to be essential for attachment of key habitat forming species, such as corals, sponges or bryozoans, that in turn can support an increase local diversity of associated fauna across the abyss, by providing substratum, refuge and increased food availability (Buhl-Mortesen et al., 2010).

Lastly, it is important to note that small-scale habitat heterogeneity also shapes benthic assemblages. For example, in soft-sedimented areas, faunal activity associated with feeding or moving on the surface and subsurface of the sediment, leads to the presence of traces on the seafloor, also designated as *lebensspuren* (Ewing and Davis, 1967). Another source of local heterogeneity in abyssal soft sediment areas relates with the presence of biogenic structures, for example from large protists (Xenophyophores), which directly provide substrata, refuge for fauna and enhance organic matter transformation processes (Levin et al., 1991; Buhl-Mortesen et al., 2010).

1.4. Mega-epifauna from the North Atlantic

The Atlantic Ocean has a mean water depth of 3730 m and complex topography (Fig.3), comprising a large variety of seafloor habitats. The North Atlantic specifically includes many relevant topographical features at abyssal depths, such as the Mid-Atlantic ridge, the Porcupine and the Madeira Abyssal Plain, and the Charlie-Gibbs, Vema and the Azores-Gibraltar Fracture Zone. These topographic features are of great interest from the biological perspective as they are known to harbour complex heterotrophic and chemosynthetic habitats, including hydrothermal vents, seepage sites, seamounts and hills.

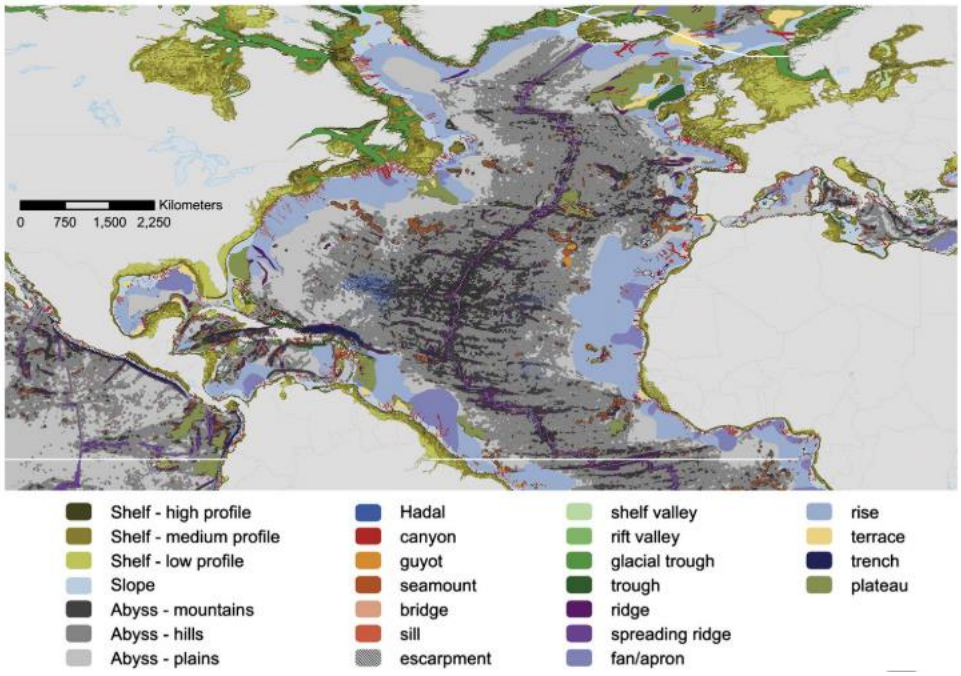

Figure 3 – Main geomorphic features of the North and Central Atlantic Ocean. From: Harris et al. (2014)

The main oceanographic regimes in the North Atlantic region are associated with the Atlantic Meridional Overturning Circulation, which consists of a northwards flow of warmer surface waters, complemented by a returning southwards flow of deeper waters, formed due to increased salinity and low temperatures (Puerta et al., 2020; Fig.4). In addition, there is recirculation within the subtropical gyre, where surface currents such as the Gulf Stream and the North Atlantic current can be identified (Puerta et al., 2020; Fig.4).

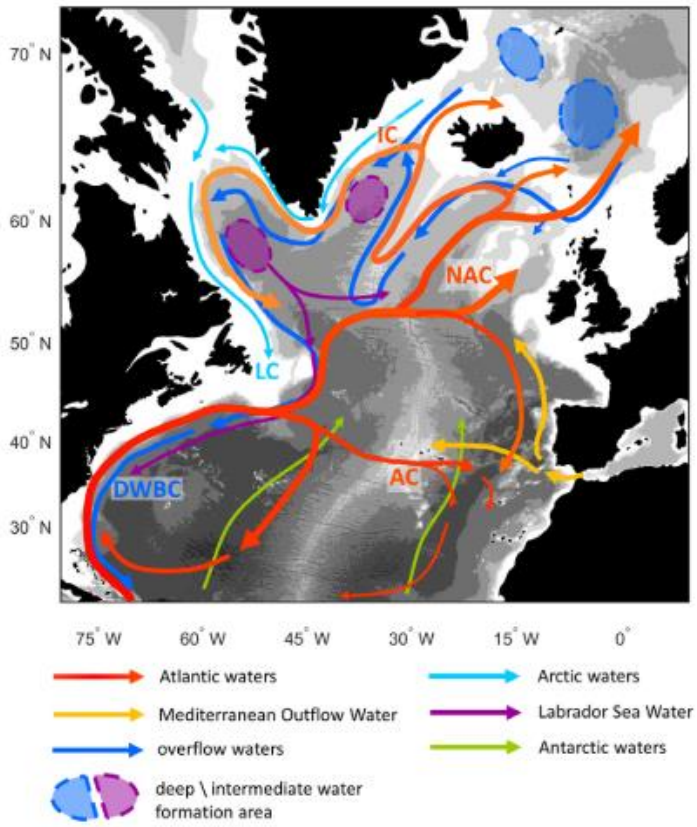

Figure 4 - Main circulation of the North Atlantic Ocean with the detail of the main currents involved: the North Atlantic Current (NAC), Azores Current (AC), Irminger Current (IC), Labrador Current (LC), and Deep Western Boundary Current (DWBC). From: Puerta et al. (2020)

With regards to deep-water masses, the abyssal North Atlantic is overall affected by the North Atlantic Deep Water, Antarctic Bottom Water (the densest water mass) and Arctic Bottom Water (Emery et al., 2001; Puerta et al., 2020). It is also important to acknowledge widespread seasonal blooms, especially associated with upwelling events in spring and early summer, can promote a substantial increase in the POC fluxes to abyssal sites, particularly near the continental margins (Tyler, 2003; Martinez et al., 2011).

The North Atlantic has been historically one of the most studied worldwide, yet due to its vastness it remains little explored, namely at abyssal depths. The current knowledge on spatial variation in mega-epifaunal community standing stocks, composition and diversity in abyssal areas is inferred from data from few sites, namely the Porcupine Abyssal Plain, Madeira Abyssal Plain and areas near the Charlie-Gibbs Fracture Zone and Mid-Atlantic Ridge (e.g., Thurston et al., 1994; Alt et al., 2019). Overall, areas studied further south, such as the Madeira Abyssal Plain, had lower mega-epifaunal density and biomass compared to the Porcupine Abyssal Plain (Thurston et al., 1994, 1998). At the Porcupine Abyssal Plain, holothurians, actinarians and asteroids are major contributors to the total abundance and

biomass, while for example at the Madeira Abyssal Plain were asteroids, natant decapods and bivalvia (Thurston et al., 1994). Moreover, abyssal sites in the Atlantic seem to have variable constituting proportions of echinoderms, where holothurians or ophiuroids are often present in high abundances (Sibuet et al., 1985 as cited in Tyler, 2002). When considering sites near the ridge and fracture zones (Charlie Gibbs Fracture Zone and Mid-Atlantic Ridge) communities were more heterogenous, with Echinodermata among the dominant taxa but other groups also present in high proportions, such as Porifera, Foraminifera and Cnidaria (Bell et al., 2016; Felley et al., 2018; Alt et al., 2019).

Noteworthy, research including comparisons a between hills and plains at Porcupine Abyssal Plain, has highlighted the importance of exploring topographical heterogeneity within each region (Durden et al., 2015; Morris et al., 2016; Durden et al., 2020b). Morris et al. (2016) and Durden et al. (2015) both detected higher mega-epifauna biomasses at hills. These mega-epifauna-related changes have been accompanied by significant higher coverage of the seabed by particulate organic matter in hills (Durden et al., 2015; Morris et al., 2016). Further differences in the composition and abundances related with small-scale variation have also surfaced at Charlie-Gibbs Fracture Zone, between flat and slope sites (Alt et al., 2019). Particularly, it was observed in the south region that suspension feeders dominated communities from slope habitats and on the contrary deposit feeders dominated communities from flat areas (Alt et al., 2019). At the level of substratum, higher species richness was observed in areas with patchier coverage of hard substratum (Bell et al., 2015).

Inter-annual variation has been evidenced with the remarkable widespread shifts in abundances recorded at Porcupine Abyssal Plain (1996-2005), specifically involving a rise in density of a holothurian species, *Amperima rosea* (Billet et al., 2001, 2010). Concerning seasonal variation, long-term observations made with the Bathysnap system have recorded seasonal deposition of phytodetritus at Porcupine Abyssal Plain, possibly affecting mega-epifauna (Billett et al.,1983; Bett et al., 2003). Nevertheless, an assessment of mega-epifauna responses to seasonal fluctuations emphasized that, for example, deposit feeding activity seemed to be taxon-specific and related to feeding and foraging modes (Durden et al., 2020a). Furthermore, time-lapse observations have also allowed to record formation of echiuran burrows, allowing improvement of density estimates, as well as enabled the study of anemones behaviours at Porcupine Abyssal Plain, and the growth of xenophyophores at the Madeira Abyssal Plain (Lampitt et al., 1987; Bett et al., 1993; Gooday et al., 1993; Rieman-Zuernek et al., 1997; Bett et al., 2003).

1.5. State of the art

Among some of the most interesting fracture zones of the Atlantic, there is the Azores-Gibraltar Fracture Zone, located in the central Northeast Atlantic and comprising both the Gloria Fault and the Southwest Iberian Margin Fault Zone (Fig.5). Even though faults are considered a risk to human societies due to their role in generating high magnitude earthquakes, the associated fracture zones are areas of interesting environmental conditions, associated for example with transportation of fluids rich in chemicals, such as hydrogen sulphide and other volatile hydrocarbons, such as methane, to the sediment surface and subsurface, which are conditions known to benefit chemosynthetic life (Hensen et al., 2019). In addition, fracture zones extensive scaring across the deep seafloor, associated to narrow valleys and steep walls (relief of more than 2000 m), produce a general complex topography reaching >5000 m water depths (Hensen et al., 2019). Noteworthy, there is an overall knowledge scarcity regarding biological communities associated to fracture zones.

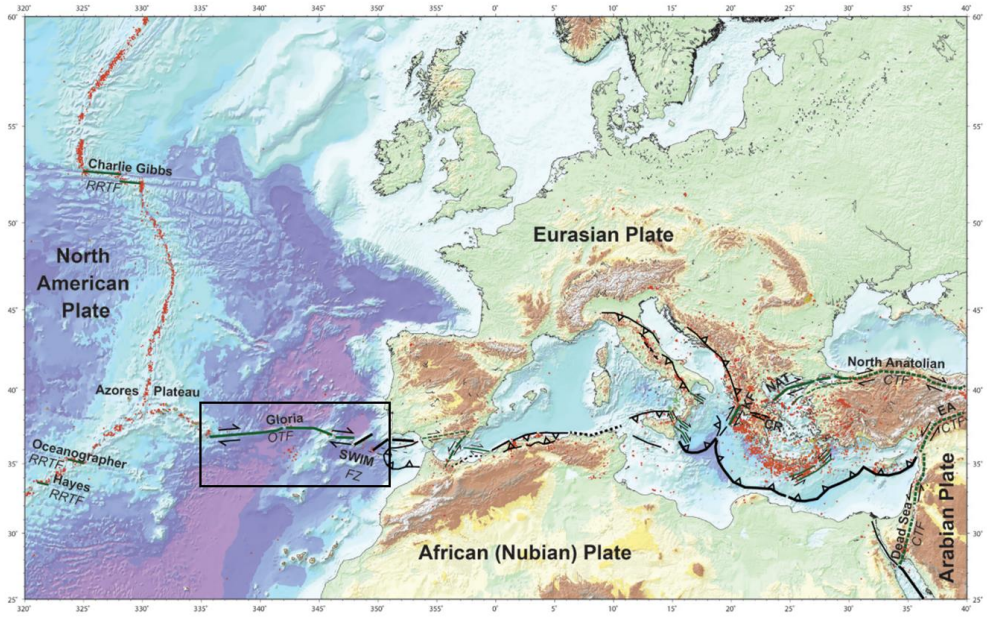

Figure 5 - Fracture zones from the Northeast Atlantic and Mediterranean regions and the location of the Azores-Gibraltar Fracture Zone, including the Gloria and southwest Iberian Margin faults. From: Hensen et al. (2020).

1.6. Main objective and hypotheses

The main goal of this study is to investigate the spatial distribution of the mega-epibenthic fauna along four main work areas of the Gloria Fault (NE Atlantic). To achieve the main goal, the following specific objectives were established: (1) quantify in each area through image-

based analyses mega-epifauna and *lebensspuren* (animal traces), which reflect the long-term activity on the seafloor; (2) compare density, composition and diversity between areas; (3) investigate the relation between the observed mega-epifaunal assemblages and large-scale variation in the environmental setting of each area; and (4) identify evidence of anthropogenic disturbance, specifically marine litter.

Considering the current knowledge on mega-epifaunal distribution patterns in abyssal regions, this study hypothesizes that the environmental differences across the four areas (e.g., varying distance to shore, varying net primary productivity, bathymetric and topographic heterogeneity, hard substrate coverage variability, fluctuations in biogeochemical parameters of water column above seafloor) will be reflected in mega-epifauna density, structural and functional composition, and structural diversity.

2. METHODOLOGY

2.1. Study area

The Gloria Fault (~800 km long) corresponds to the central domain of the Azores-Gibraltar Fracture Zone, which crosses the northeast Atlantic (starting at the Azores plateau and extending to the Strait of Gibraltar), establishing the tectonic boundary between the African/Nubia and Eurasian plates (Hensen et al., 2019; Omira et al., 2019). Formerly, on the eastern continuation, the Azores-Gibraltar Fracture Zone has been associated to various seepage sites in the Horseshoe Abyssal Plain and Gulf of Cadiz, including mud volcanoes with active fluid flow rich in methane (Hensen et al., 2007, 2015, 2019).

The Gloria Fault possesses a prominent morphological expression, spreading between the eastern tip of the Terceira Rift (Azores), where recent evidence indicates ongoing hydrothermal activity (Schmidt et al., 2019), and the Josephine seamount, part of the Madeira Tore Rise geological complex (Omira et al., 2019). Geomorphologically, it has been described as a 15 - 20 km wide depression with vertical offsets of more than 1 km, comprising E-W elongated basins and ridges and reaching depths up to 6000 m (Omira et al., 2019). Covering the oceanic crust of the Gloria Fault there is a layer composed predominantly by hemipelagic sediments, interbedded with gravity-driven sediment deposition and basaltic outcrops (Batista et al., 2017; Omira et al., 2019). In terms of seismic activity, the Gloria Fault has a relatively slow inter-plate motion and dominantly exhibits a dextral strike-slip faulting, but comprises three distinct segments with varying predicted slip rates (from 3.2 $mm.yr^{-1}$ and 2.0 $mm.yr^{-1}$) and variable seismic activity: (1) western Gloria, a 300 km long segment, initiating at the tip of the Terceira rift, located between 24°W and 19°30W and striking WSW - ENE, (2) central Gloria, a 150 km long segment, located between 19°30W and 18°W and striking SW - NE and

(3) eastern Gloria, a 250 km long segment, located between 18°W to 14°30W, striking WNW - ESE and culminating at the Josephine seamount (Omira et al., 2019; Fig.6). Seismic activity of the central and eastern Gloria Fault has already been marked by large earthquakes of magnitude greater than 7.0 and predictions for the western segment indicate fault locking and loading which may result in future strong earthquakes (Omira et al., 2019).

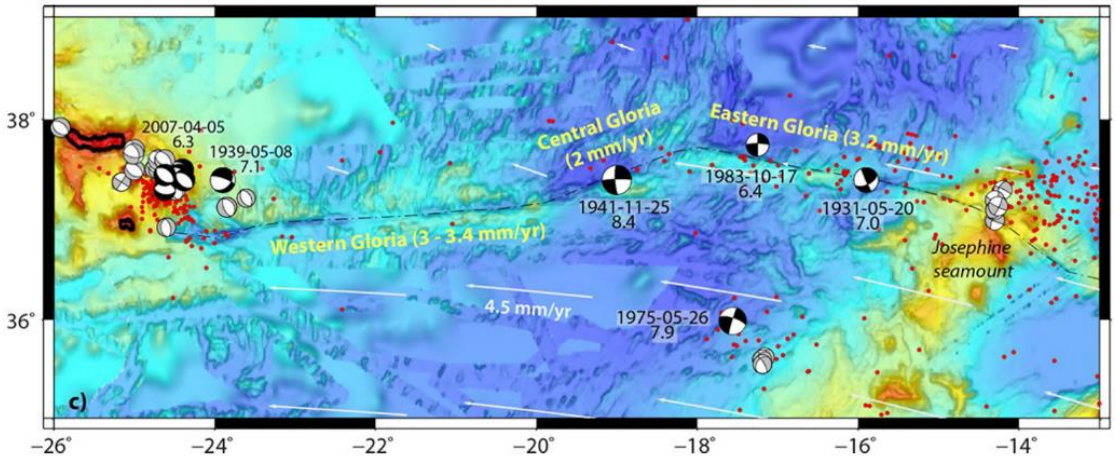

Figure 6 - Gloria Fault main segments and corresponding varying predicted slip rates and seismic activity. From: Omira et al. (2019).

The large-scale surface circulation above the Gloria Fault region is under the influence of the North Atlantic Subtropical Gyre, which involves the Gulf Stream, the Azores, the Portugal and the Canary currents (Barton, 2001; Caldeira and Reis, 2017). Specifically affecting the region there is the eastward flow of waters under the Azores Current, fed by the Gulf Stream, which brings warm waters from the south (Barton, 2001; Caldeira and Reis, 2017). Noteworthy, the Azores region is affected by several eddies originating both from the Gulf Stream and the Azores Current (Caldeira and Reis, 2017).

Regarding the main water masses that influence the region, the Eastern North Atlantic Central Water and Mediterranean Outflow Water, entering from the Strait of Gibraltar, predominantly influence the upper and intermediate layers (above 1500 m) (Liu and Tanhua, 2021). Noteworthy, associated to the outflow of Mediterranean water there is the formation of meddies at the Gorringe Bank, as it is an elevated area part of the Madeira-Tore complex (Serra and Ambar, 2002). At depths ranging between 2000 and 4000 m, the predominant water mass is the North Atlantic Deep Water (NADW), while below 4000 m water depth, the Northeast Atlantic Bottom Water predominates (Liu and Tanhua, 2021). The

resulting water conditions below 2000 m include average temperatures ranging between 1.95 and 3.33 ºC, oxygen concentrations ranging between 245 to 280 µmol.l^{-1}, and a constant salinity of 35 (Liu and Tanhua, 2021).

2.2. Imagery and environmental data collection

During the cruise M162 (March - April 2020) on board of R/V Meteor, a series of systematic and multidisciplinary surveys were conducted along the main trace of the Gloria Fault (Hensen et al., 2020). This cruise aimed overall to identify the presence of fluid flow structures along the Gloria transform fault, investigating both the relationship between fluid flow and seismic activity, as well as the potential spread of seepage habitats (Hensen et al., 2020).

Table 1 – Overview of sampling stations information on position (start and end site), transect length, depth ranges, extracted and used still images and total annotated area.

Station	Work area	Region	Start site		End site		Length (m)	Depth (m)	Extracted/ used images	Area (m^2)
			Latitude (Nº)	Longitude (Wº)	Latitude (Nº)	Longitude (Wº)				
VCTD1	WA01	Terceira rift	37°58.048	26°05.252	37°57.533	26°06.234	4040	3153-3180	1512/416	462
VCTD2	WA02	Western Gloria	37°19.658	21°20.207	37°20.952	21°20.324	2410	4120-4124	966/310	489
VCTD3			37°03.525	21°18.734	37°05.121	21°18.729	2820	4185-4500	1426/217	325
VCTD4			37°04.590	21°17.314	37°04.571	21°18.809	2200	4448-4540	1417/299	356
VCTD5	WA04	Central Gloria	37°29.207	18°40.285	37°30.310	18°40.040	2090	4500-4718	827/194	185
VCTD6			37°27.866	18°24.898	37°27.778	18°25.838	1400	4613-4650	551/83	48
VCTD7	WA06	Eastern Gloria	37°14.477	14°54.947	37°14.765	14°55.658	1130	3515-3520	512/269	139

During the expedition, exploratory imagery transects and associated environmental data collection were carried using the water sampler rosette/video-guided CTD system (VCTD; Fig.8), deployed in four work areas along the main trace of the Gloria Fault at: (1) Terceira rift, in the tip of the Gloria Fault (WA01), (2) western Gloria segment (WA02); (3) central Gloria segment (WA04) and (4) eastern Gloria segment, near the Madeira-Tore Rise (WA06) (Table 1; Fig.7). In total, seven sampling stations were surveyed at depths ranging from 3150 and 4720 m, varying in total transect length (1130 - 4040 m) and bottom observation times (70 - 250 min; Table 1).

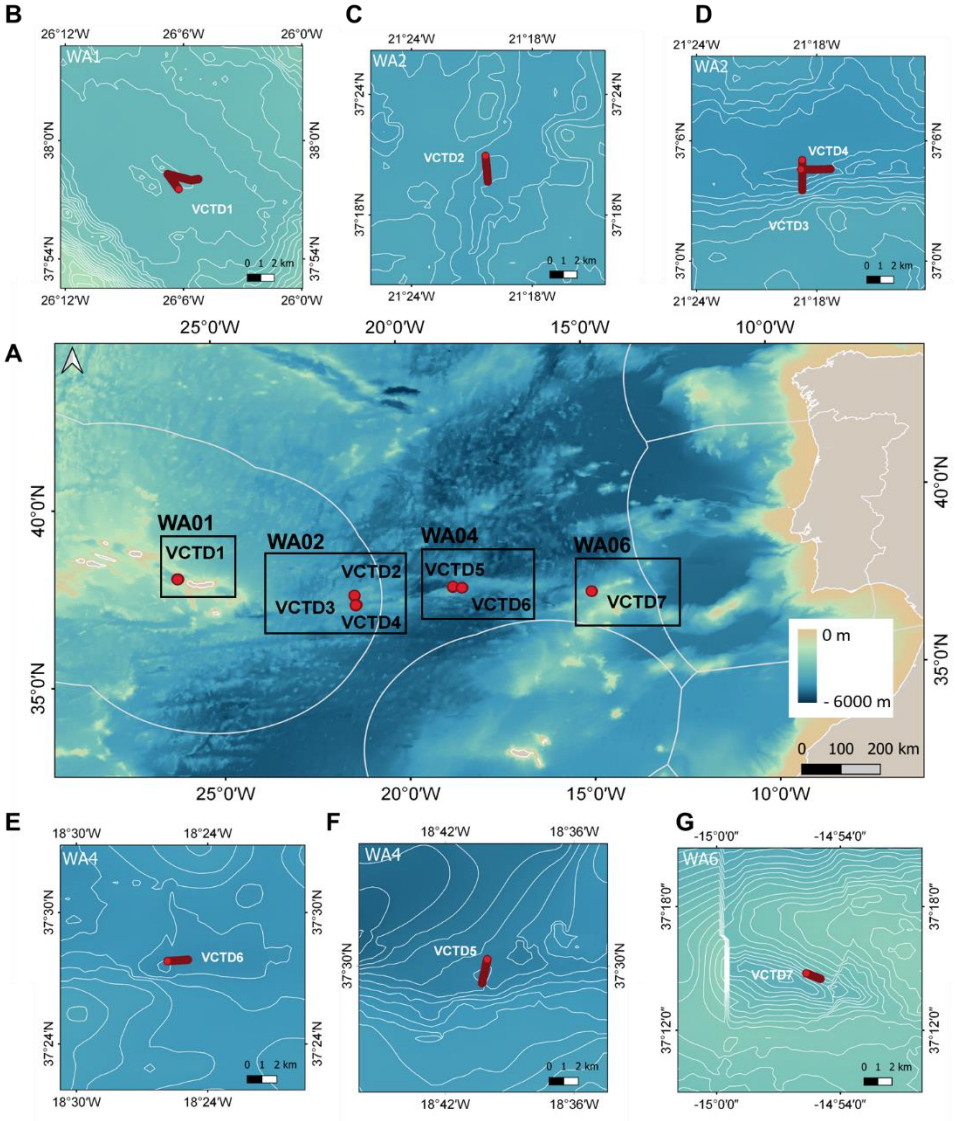

Figure 7 - (A) Overview of the work areas and sampling stations locations along the Gloria Fault and close up of **(B)** WA01, located in the Terceira rift, **(C and D)** WA02, located in the western segment of the Gloria Fault **(E and F)** WA04, located in the central segment of the Gloria Fault and **(G)** WA06, located in the eastern segment of the Gloria Fault near the Madeira Tore Rise.

During each deployment, the VCTD system was towed at a speed of 0.5 kn (approximately 0.3 m.s^{-1}). The frame was equipped with a high-definition video camera and light sources attached to the lower part of the frame, and was controlled by telemetry, pressure and altimeter readings, as well as real-time seafloor video monitoring from the ship, using a rope length as reference (Fig.8). In addition, the frame was equipped with varying sensors, including the CTD (SBE9plus, Sea Bird Eletronics), O_2 and turbidity profilers (Chelsea Nephelometer), methane sensors (Contros) and an altimeter sensor, recording all measurements every second, including water depth (m), temperature (ºC), oxygen

concentrations (µmol.l^{-1}), salinity, methane concentrations (ppm) and turbidity (FTU), and positioning data.

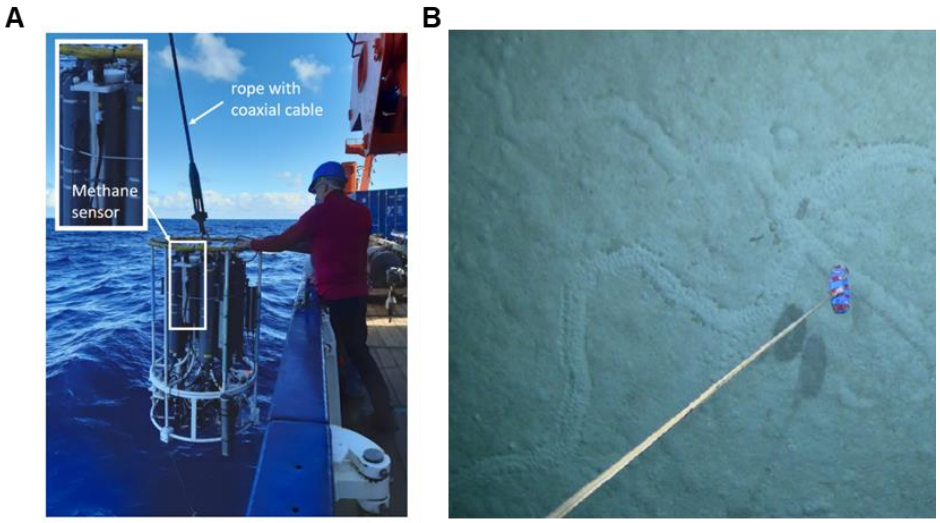

Figure 8 – (A) Video-guided CTD system and location of the methane sensor and **(B)** image example showing the guiding rope used to control distance from the seafloor and the weight used as scale (12 cm width). From: Hensen et al. (2020)

2.3. Net primary production

In addition to environmental variables measured during the cruise, surface productivity was estimated using satellite-derived information. The modelled average monthly Net Primary Production measurements (NPP, mgC.m^{-2}.day^{-1}) from the 12 months prior to sampling, were acquired from the Ocean Productivity Database from Oregon State University (geotiff files with a grid size 2160x4320 and file units mgC.m^{-2}.day^{-1}). The NPP values from the model available in the Ocean Productivity Database are calculated following the Vertically Generalized Production Model (VGPM) algorithm, originally described by Behrenfeld and Falkowski (1997), based on observations of surface chlorophyll concentrations, sea surface temperatures and daily photosynthetically active radiation from MODIS aqua (Moderate Resolution Imaging Spectroradiometer). Using QGIS (v3.10.14; http://qgis.osgeo.org), monthly NPP values were extracted based on the positions recorded during each imagery surveys transect conducted at sampling stations. In addition to the NPP values, seasonal temporal fluctuations in surface productivity were assessed with the Seasonal Variation Index (SVI), by dividing of standard deviation of the NPP monthly value by their average, as described in Lutz et al. (2007).

2.4. Imagery annotation

The annotation of the imagery aimed at both the description and identification of the seafloor substrate types, as well as the quantification of all observed mega-epifaunal organisms, animal traces and any evidence of anthropogenic disturbance (i.e., marine litter). To assist imagery annotation, all videos and still images were first visualized and a catalogue of all different seafloor substrate types, morphological distinct organisms (from here on designated as morphospecies) and different *lebensspuren* (meaning 'life traces'; Ewing and Davis, 1967) was created. To be able to conduct quantitative analyses on the imagery acquired, still images were extracted from the video recordings every ten seconds. The conservative interval permitted to avoid loss of area surveyed, while avoiding also major overlap. The quantitative annotations were conducted on the extracted still images using the software Paparazzi (v2.0) (Marcon and Purser, 2017) and during the annotations, each image file was classified in terms of its quality based on camera altitude, using a scale ranging from 0 to 3 (0 - too close to the seafloor, unusable; 1- low altitude, resulting in a clear image where all features could be seen clearly; 2 - higher altitude, resulting in a darker edges of the image, but main features could still be identifiable; and 3 - too far from the bottom, unusable). Only images classified as usable (1 and 2) where major overlaps in relation to previous images could not be seen, were annotated. The annotation procedure included an initial image correction in terms of brightness, contrast and gamma parameters, definition of the usable area (i.e., excluding blurred and dark corners, as well as overlapping sections if applicable), setting the scale (12 cm) using the reference object, and finally annotation of all visible morphospecies, faunal traces or litter. During the annotation procedure, the seabed type was also recorded for each image file following the classification mentioned below (more details provided in section 2.4.1.).

Regarding the image corrections, intervals were defined for brightness, contrast and gamma parameters, for consistency purposes. For images classified as usable with a quality/altitude 1, the brightness was adjusted between 0 and 5, contrast between 10 and 15 and gamma between 10 and 20, and for images classified as usable with a quality/altitude 2, brightness was adjusted between 5 and 10, contrast between 10 and 20 and gamma between 10 and 15. Furthermore, due to the absence of a scale for VCTD1, a usable area was estimated *a posteriori* based on calculated averages per each image quality/altitude class usable (either 1 or 2).

Finally, each image was associated with the dive metadata information (e.g., sampling station, work area, positioning, etc) as well as environmental variables registered during the dives, and productivity data acquired.

2.4.1. Seabed substrate type classification

The seafloor substrate type was described and categorized for each image based on its composition, namely in terms of varying proportions of soft and hard substrata. Main categories included: 1) Muddy sediments; 2) Mixed substrata, which were characterised by a varying percentage of both soft sediments and hard substrata; and 3) Vertical walls, which were typically covered by muddy sediments (Fig.9). Furthermore, for each category, small differentiations were also included in the descriptions. For example, if muddy sediment areas exhibited overall smooth surface, evident bioturbation or sparse presence of dark patches or even yellow patches, which could indicate reduced conditions (Fig.9a-c). For mixed substrata, all areas had predominantly muddy coverage but were sometimes interrupted by the present of small nodules (Fig.9d), or sparce boulders or basalts outcrops (Fig.9e-f). Vertical walls were also mostly covered in muddy sediments (Fig.9g), but in some cases, evidence of basalts was also observed (Fig.9h).

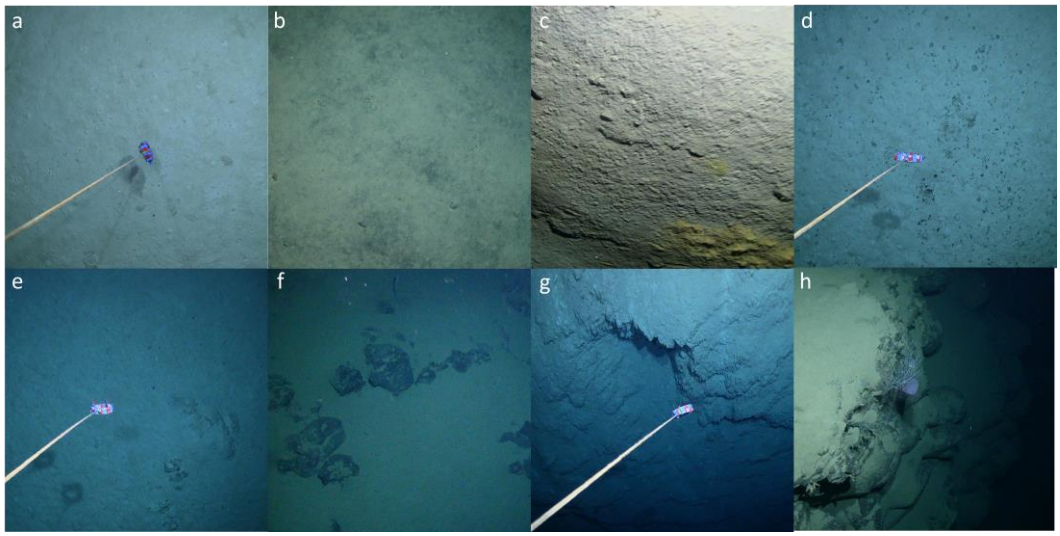

Figure 9 - Examples of substrate types observed along the Gloria Fault, including examples of muddy sediments (a-c), mixed substrata (d-f) and vertical walls (g-h).

2.4.2. Fauna and lebensspuren identification and annotation

The quantitative annotation and identification of faunal organisms and *lebensspuren* per image was conducted, as much as possible, to the morphospecies and trace type level, using the previously prepared catalogues with examples of the main groups, their different morphospecies listed and trace or detritus types (e.g., Fig.10 and 11). In some cases, namely when image quality would not allow the accurate identification of a specimen, higher taxonomical level was attributed to that specimen, and whenever such was not possible, the specimen was classified as an unidentified animal (Animalia indet).

The fauna included in the catalogues were identified to the lowest taxonomical level possible using information from published catalogues, databases and relevant literature (e.g. Benthic Deepwater Animal Identification Guide from NOAA Ocean Exploration; Howell et al., 2017; Oliveira et al., 2017), but often identifications were restricted to class or order level, due to the lack of physical specimens for comparison and needed to support a more precise identification.

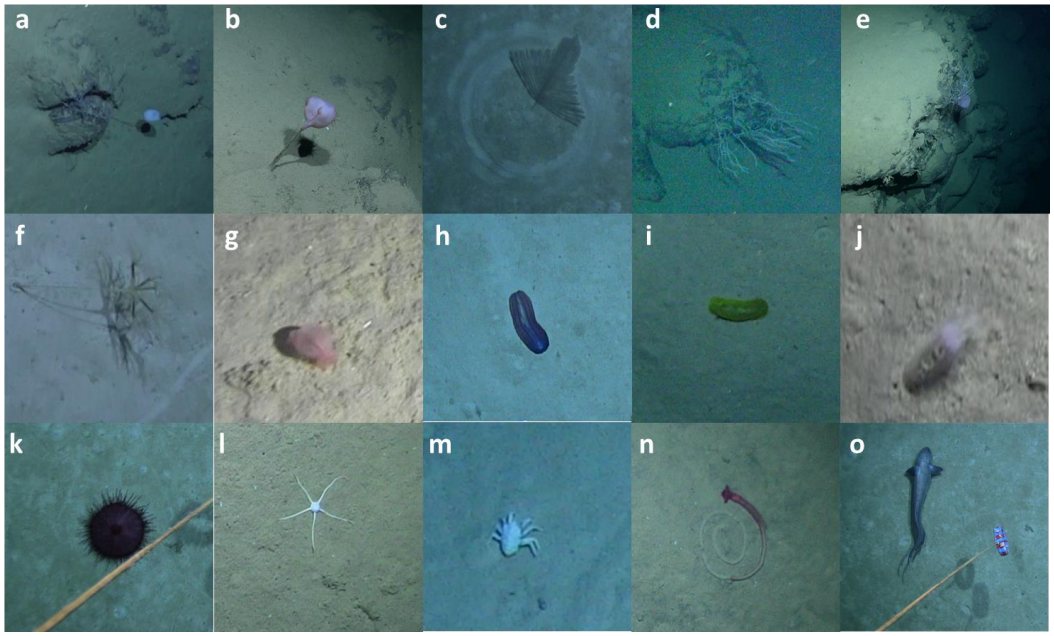

Figure 10 – Observations across the Gloria Fault of the main taxa, including (a) Porifera, (b) Actiniaria, (c) Antipatharia, (d) and (e) Alcyonacea, (f) Pennatulacea, (g-j) Holothuroidea, (k) Echinoidea, (l) Ophiuroidea, (m) Galatheidae, (n) Enteropneusta and (o) Actinopterygii.

Once the dive was fully annotated for fauna, *lebensspuren* and marine litter, the results were exported, providing information on the usable areas (m^2), morphospecies and traces counts, as well as density ($ind.m^2$). In the case of finding morphospecies in images classified as unusable or in areas outside the defined usable area, their presence was still recorded (but not annotated on the software) in order to assess the missed taxa through the quantitative annotation's procedure. Additionally, all video recordings were also previewed to record possible missed taxa during the quantitative annotations.

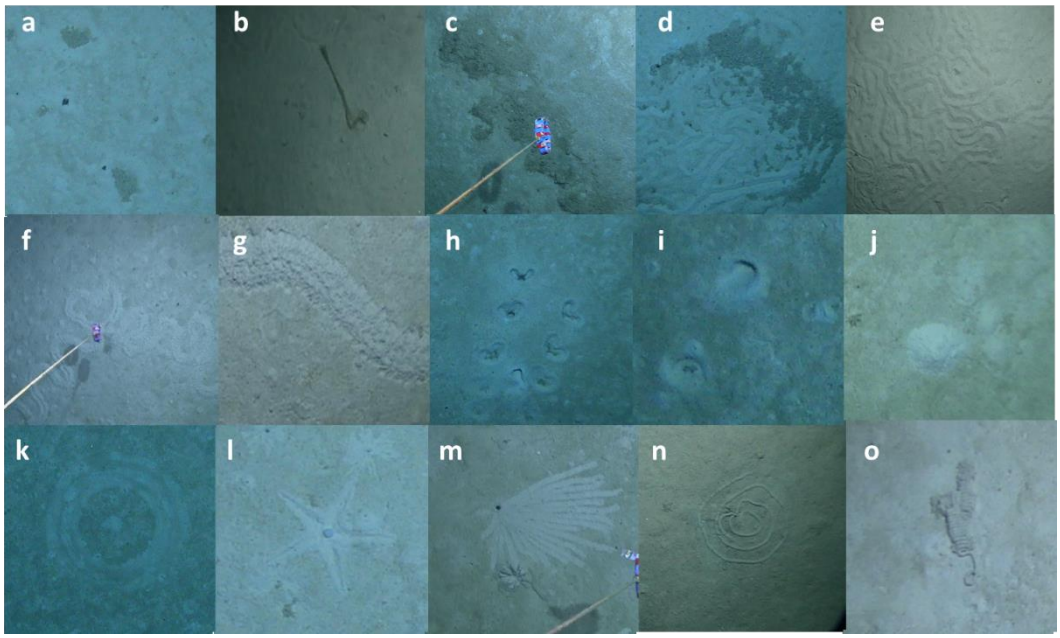

Figure 11 – Different detritus and *lebensspuren* observations across the Gloria Fault, including detritus (a-c), locomotion tracks (d-g), burrows and mounds (h-j) and feeding and foraging traces (k-o).

2.5. Functional trait analysis

In addition to taxonomic identification of the specimens observed, morphospecies encountered were also classified in terms of their functional aspects by means of a traits approach, which included the classification of their motility, feeding mode and tiering traits. These three traits were the only which could be confidently scored, due to difficulties in assigning functional aspects to abyssal mega-epifauna associated with the lack of supporting literature. The trait motility was included to assess the dispersal potential of organisms within the ecosystem, influencing the organisms access to food, the foraging behaviour and ability to escape predation, as well as to relocate in response to environmental changes; the feeding mode to assess the variety of behaviours when exploiting different types of food resources and tiering as it is related with the physical space occupied by the fauna within the ecosystem (Costello et al., 2015; Chapman et al., 2019; Nunnally et al., 2020; Marine Species Traits editorial board, 2021). Different modalities were then attributed to each of these traits (Table 2). For mobility, morphospecies were either assigned as sessile, discretely motile or motile; for feeding mode as deposit feeder, suspension feeder, detritivore/scavenger and predator; and for tiering as benthopelagic, epibenthic and infauna (Table 2).

Table 2 – Functional traits categories and modalities analysed for the mega-epifauna.

Traits	Modality	Description
Mobility	Sessile	Completely sessile
	Discretely motile	Able to move, but for short distances
	Motile	Movement (medium/long distances) is required for feeding
Feeding mode	Deposit feeder	Feeds on fragmented particulate organic matter (POM) ingesting sediment together
	Suspension feeder	Feeds on POM by catching food on a filter, by actively sweeping or pumping, or by collecting detritus on sticky apparatus
	Detritivore/Scavenger	Actively feeds on dead organic material (animal or decaying surface plant material)
	Predator	Feeds by preying on other organisms, killing/capturing prey capable of resisting
Tiering	Benthopelagic	Living in the water column, free from the bottom or living at or near the bottom, but having the capacity for actively swimming
	Epibenthic	Living on the surface of the substratum, not extending significantly upwards
	Infauna	Living in the subsurface of the substratum

2.6. Data analyses

The descriptive analysis of the environmental setting was performed based on a data set including the following variables: water depth (m), temperature (ºC), oxygen concentrations (µmol.l^{-1}), salinity, methane concentrations (ppm), turbidity (FTU), average monthly Net Primary Productivity (NPP, mgC.m^{-2}.day^{-1}) and Seasonal Variation Index (SVI). With regards to the biological dataset, fauna and traces observations were expressed, respectively, as individuals and traces per square meter (ind.m^{-2} and traces.m^{-2}), calculated based on counts and usable areas resulting from annotations.

All statistical analyses of both environmental and biological datasets were performed with the software PRIMER (v7) and PERMANOVA+ (Anderson et al., 2008; Clarke and Gorley, 2015). In order to detect significant differences between work areas in terms of mega-epifaunal densities and composition, respectively uni- and multivariate analysis were performed. For both cases, the analysis of variance was explored using random permutations method (PERMANOVA), with a 2-factor design (“Work area” as a fixed factor and “Sampling stations” as a random factor nested in “Work area”). For cases where the number of permutations was low, the Monte-Carlo p-values were used in detriment of the permutational p-values. Prior to

each PERMANOVA test and due to its sensitivity to dispersion effects within groups, a test of homogeneity of dispersions (PERMDISP) was also performed.

To investigate the differences in the environmental setting across the different work areas data, the PERMDISP and PERMANOVA tests were applied to a Euclidean distances matrix after data was normalised and fourth root transformed. This procedure was followed by a Principal Component Analysis (PCA) performed to explore the differences in the environmental setting across work areas, considering the investigated environmental variables.

To test differences in total mega-epifaunal densities across work areas, the PERMDISP/PERMANOVA routines were applied to Euclidean distance matrixes. The same procedure was followed for total *lebensspuren* densities. The individuals which were assigned as motile taxa capable of actively swimming were excluded from the total density analysis performed, but the ones which remained unassigned to specific taxa were included.

To investigate the patterns in composition of mega-epifauna across sampling stations and work areas, a Non-Metric Multidimensional Scaling (nMDS) ordination was conducted, using both the faunal replicate data matrix (observations per still image), as well as fauna data matrix pooled per sampling station. Prior to the nMDS ordinations, a Bray-Curtis similarity matrix was calculated after the application of the fourth root transformation. This procedure was followed by a PERMDISP and PERMANOVA analysis to detect significant differences. Afterwards, to determine the relative contribution of each morphospecies to (dis)similarities between the main work areas, a Similarity Percentage Analysis Procedure (SIMPER) was performed. Noteworthy, the data set analysed in PRIMER excluded all images where no mega-epifaunal observations existed, as the software is unable to compute similarities when a total absence of observations is verified. In this analysis, the individuals which were assigned as motile taxa capable of actively swimming were excluded, along with the ones which remained unassigned to specific taxa.

To explore the relationship between mega-epifauna structural composition and the environmental setting of the investigated work areas, a Distance-Based Linear Model (DISTLM) analysis was performed, using adjusted R^2 as a selection criterion, followed by the computation of a Distance-Based Redundancy Analysis (dbRDA) plot to illustrate the DISTLM model.

The investigation of mega-epifaunal structural diversity at morphospecies level was conducted based on the calculation of several indices: Species Richness (S), Pielou's Evenness (J'), Shannon-Wiener (H'), and the following Hill Numbers: N_1, as a transformation of the Shannon diversity; N_2 as the inverse Simpson and $N\infty$ as the reciprocal of the Berger-Parker index, as a diversity index also reflecting dominance. In addition, the Hurlbert (1971)

Expected Species Richness ($ES_{(n)}$) based on the number of individuals (n) were also calculated to plot the rarefaction curves for each sampling station, work area and in total. In the diversity analysis, the individuals which were assigned as motile taxa and capable of actively swimming were also excluded, along with the ones which remained unassigned to specific taxa.

In addition, the diversity partitioning was assessed for both Species Richness (S) and Shannon-Wiener (H'), as followed by Crist et al. (2003), carrying the partitioning by weighting each sample by abundance (Crist et al., 2003). Specifically, the total diversity (γ) was partitioned into the average diversity within images/samples (α) and among images/samples (β), and therefore β-diversity was estimated by $\beta = \gamma - \alpha$, knowing that $\gamma = \alpha + \beta$ (Wagner et al., 2000). The partition was also extended across different scales with β1 referring to diversity within sampling stations, β2 referring to diversity between sampling station and β3 referring to diversity between work areas. The smallest sample unit for level 1 corresponded to annotated images, while for the upper levels the sampling units corresponded to pooling together groups of samples/still images. The respective diversity components were calculated as $\beta_m = \gamma - \alpha_m$ at the highest level (3) and $\beta_i = \gamma - \alpha_{i+1} - \alpha_i$ for each lower level (1 and 2). The additive partition of diversity corresponded to $\gamma = \alpha_1 + \beta_1 + \beta_2 + \beta_3$ and the resulting total diversity was therefore expressed as the percentage contributions of diversity in each hierarchical level (Crist et al., 2003).

3. RESULTS

3.1. Variation of the environmental setting along the Gloria Fault

The summary of measured environmental variables per sampling station and work area is provided in detail in Table 3. The highest values of environmental variables, except turbidity and methane concentrations, were consistently observed at Terceira rift (WA01). The depths surveyed at WA01 corresponded to 3185±28.1 m and temperatures and oxygen concentrations were respectively 4.7±0.00 °C and 258.86±0.793 µmol.l^{-1}. On the contrary, the work areas at western (WA02) and central Gloria (WA04) were the deepest surveyed (4324±173.0 and 4662±47.8 m) and consistently presented the lowest temperatures and oxygen concentrations (2.56±0.006 and 2.46±0.010 ºC; 244.48±0.933 and 244.79±0.612 µmol.l^{-1}). The second highest values were observed at eastern Gloria, near the Madeira Tore Rise (WA06) (3517±9.7 m, 2.9±0.00 °C and 248.53±2.177 µmol.l^{-1}). The net primary productivity (NPP) and the seasonal variation index (SVI) was respectively 553.89±0.000 mgC.m^{-2}.day^{-1} and 0.28±0.000 at WA01, while the remaining work areas

(WA02, WA04 and WA06) had NPP values ranging between 379.21±0.000 and 430.14±3.687 $mgC.m^{-2}.day^{-1}$, and SVI values ranging between 0.13±0.000 and 0.16±0.002. In terms of salinity, no changes were observed between work areas. The turbidity levels at WA06 were respectively, 19 and up to 316 times higher (27.88±0.000 FTU), than the values observed at WA01 (1.47±0.055 FTU), and at WA02 and WA04 (0.09±0.002 and 0.09±0.003 FTU, Table 3). On the contrary, methane concentrations observed at WA06 (0.10±0.001 ppm) were up to 24 times lower than at other work areas (ranging between 2.18±0.320 and 2.32±0.202 ppm, Table 3).

Table 3 – Average ± standard deviation of environmental parameters measured at each sampling station and work area, including surface Net Primary Productivity (NPP) and Seasonal Variation Index (SVI).

Sampling station	**Depth** (m)	**Temperature** (°C)	**Oxygen** ($\mu mol.l^{-1}$)	**Salinity**	**Methane** (ppm)	**Turbidity** (FTU)	**NPP** ($mg.C.m^{-2}.day^{-1}$)	**SVI**
VCTD1	3185±28.1	4.7±0.00	258.86±0.793	35.0±0.00	2.32±0.202	1.47±0.055	553.9±0.00	0.28±0.000
VCTD2	4117±1.7	2.6±0.00	244.86±0.806	34.9±0.00	2.34±0.257	0.09±0.001	402.2±0.00	0.16±0.000
VCTD3	4401±87.0	2.6±0.01	244.18±0.763	34.9±0.00	2.04±0.283	0.09±0.003	390.7±0.00	0.16±0.000
VCTD4	4484±54.3	2.6±0.01	244.32±1.036	34.9±0.00	2.42±0.185	0.09±0.001	390.8±0.22	0.16±0.002
VCTD5	4662±56.5	2.5±0.01	244.70±0.643	34.9±0.00	2.09±0.313	0.09±0.001	432.5±0.00	0.14±0.000
VCTD6	4662±13.8	2.4±0.00	245.01±0.464	34.9±0.00	2.37±0.245	0.10±0.002	424.5±0.00	0.17±0.000
VCTD7	3517±9.7	2.9±0.00	248.53±2.177	34.9±0.00	0.10±0.001	27.88±0.000	379.2±0.00	0.13±0.000
WA01	3185±28.1	4.7±0.00	258.86±0.793	35.0±0.00	2.32±0.202	1.47±0.055	553.9±0.00	0.28±0.000
WA02	4324±173.0	2.6±0.01	244.48±0.933	34.9±0.00	2.29±0.287	0.09±0.002	395.0±5.53	0.16±0.002
WA04	4662±47.8	2.5±0.01	244.79±0.612	34.9±0.00	2.18±0.320	0.09±0.003	430.1±3.68	0.15±0.013
WA06	3517±9.7	2.9±0.00	248.53±2.177	34.9±0.00	0.10±0.001	27.88±0.000	379.2±0.00	0.13±0.000

Overall, the environmental variables investigated apparently differed significantly between work areas ($p<0.01$; Annex Table A2 and Table A3), but significant PERMDISP test results suggested variability within work areas ($p<0.01$; Annex Table A1). Nevertheless, differences among work areas were evident in the Principal Component Analyses (PCA) plot (Fig.12). The WA02 and WA04 are shown separated from WA01, indicating overall differences in depth, temperature, oxygen concentrations, salinity, NPP and SVI (Fig.12). Moreover, the separation shown also reflected the differences in methane concentrations and turbidity, which were respectively, the lowest and the highest at WA06 (Fig.12).

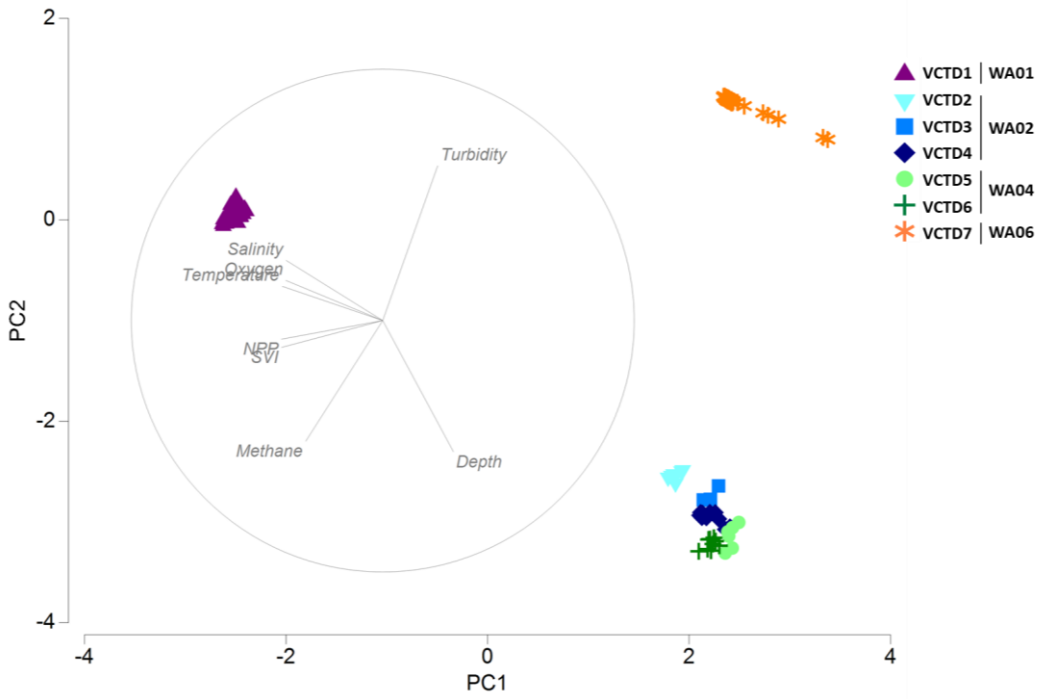

Figure 12 - Principal Component Analysis (PCA) plot based on environmental variables displaying the dispersion of observations**.**

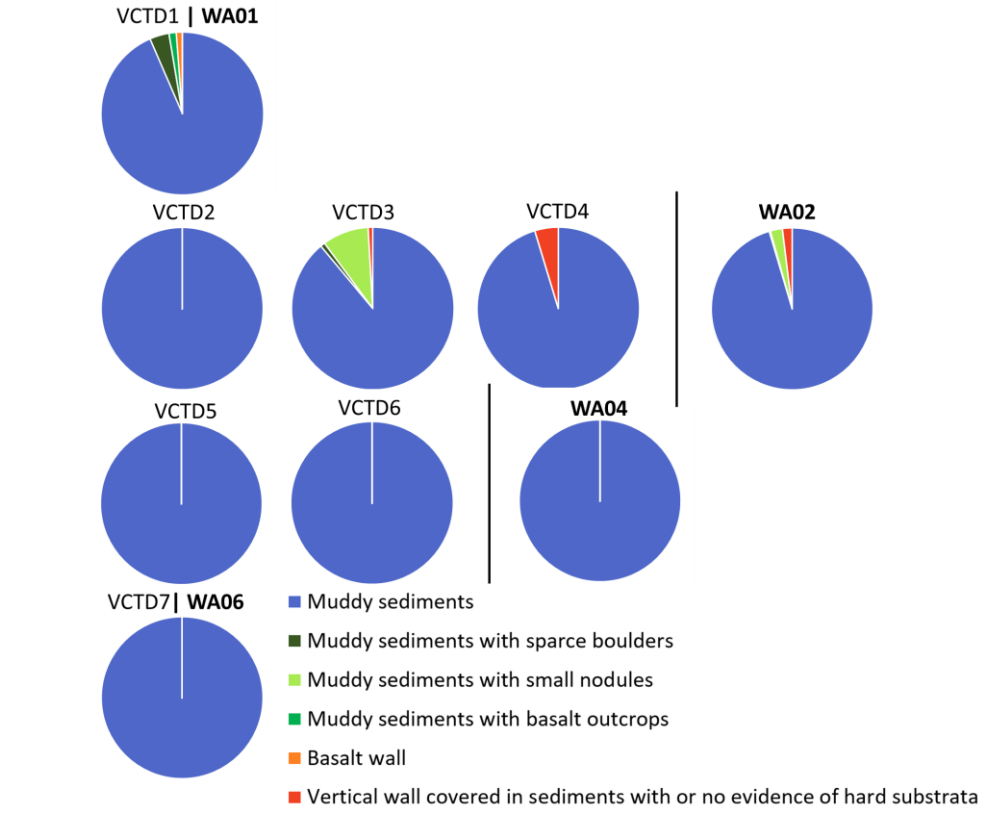

Figure 13 - Seabed type composition of each sampling station and corresponding work areas.

In addition to the variables measured during the CTD deployments, the visual assessment of seafloor seabed type revealed a general dominance of muddy sediments along the Gloria Fault (Fig.13). The WA01 presented the largest variety of substrate types, followed by WA02. On the contrary, the WA04 and WA06 were exclusively composed of muddy sediments (Fig.13).

3.2. Mega-epifauna from the Gloria Fault

3.2.1 Density

A total of 383 individuals were annotated in still images from imagery transects conducted along the Gloria Fault, of which 309 were assigned as epifaunal taxa, 33 as mobile taxa and 41 remained unassigned to a specific taxon due to low resolution of images. The motile taxa could not be confidently quantified due to their ability to avoid or be attracted by the light system, hence they were descriptively analysed separately.

The average density at the eastern Gloria near the Madeira Tore Rise (WA06), was approximately 2 times higher (0.87±1.513 ind.m^{-2}) when compared to Terceira rift (WA01, 0.38±0.876 ind.m^{-2}), and at least 10 times higher by comparison to both western and central Gloria (WA02 and WA04, 0.04±0.038 and 0.09±0.089 ind.m^{-2}, respectively) (Fig.14A). There was generally a high variability in density within work areas, namely within WA04, where VCTD6 presented an average density about 5 times higher (0.21±0.622 ind.m^{-2}) by comparison to VCTD5 (0.04±0.206 ind.m^{-2}) (Fig.14A). The significant PERMDISP results ($p<0.01$; Annex Table A4) suggested variability within work areas and therefore no significant differences between work areas could be confidently assigned (Annex Table A5). With regards to motile taxa density, densities varied little between work areas (ranging between 0.003±0.0033 ind.m^{-2} and 0.026±0.1505 ind.m^{-2}, WA01 and WA04, respectively; Fig.14B).

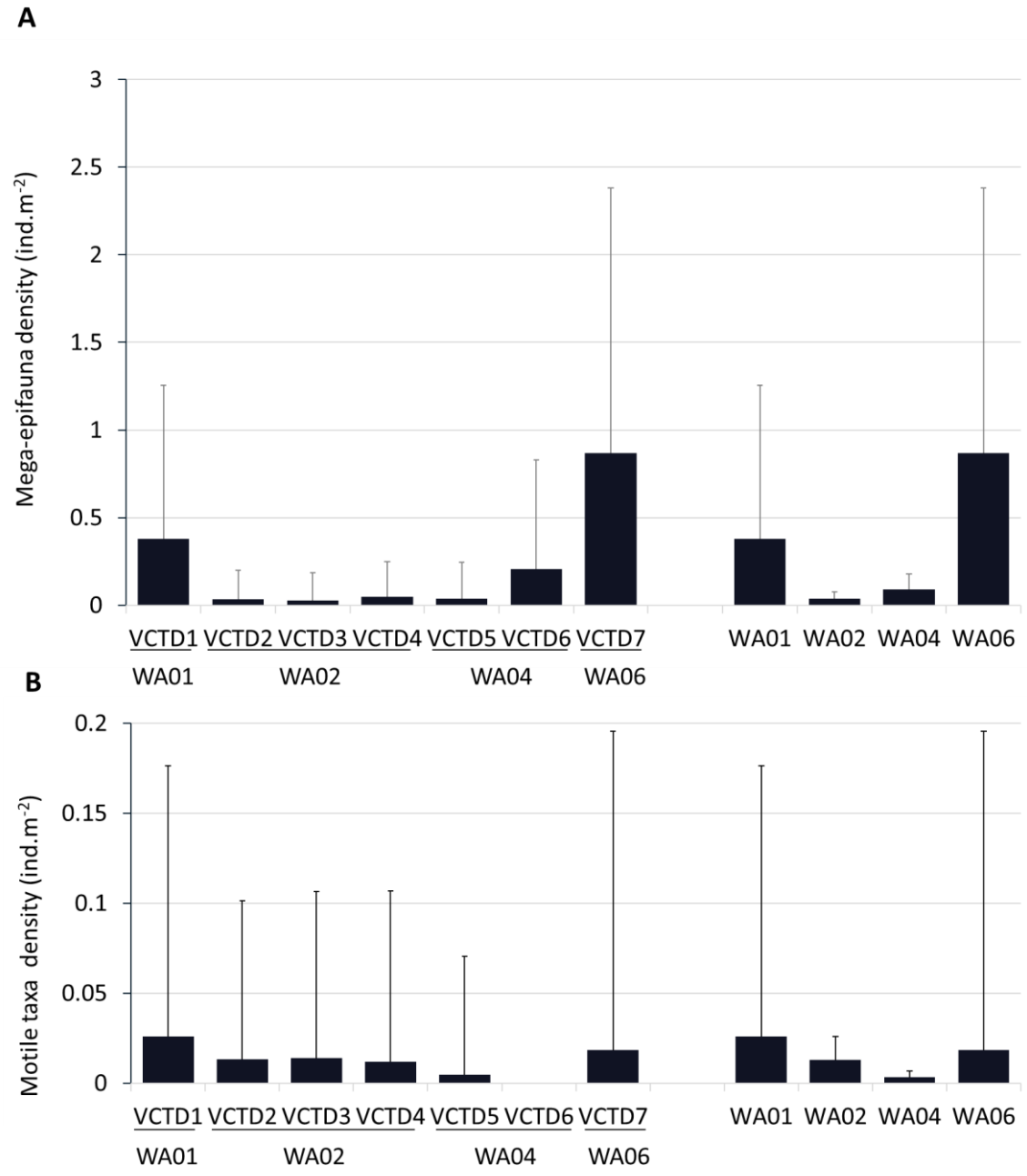

Figure 14 - Average density ± standard deviation (ind.m^{-2}) of **(A)** mega-epifauna excluding motile taxa and **(B)** motile taxa alone per sampling station and work area.

3.2.2. Composition

The qualitative assessment based on all imagery acquired, including video observations and excluded sections of annotated image stills, revealed a total of 79 different mega-epifauna morphospecies (Table 4). In contrast, the quantitative analysis based only on extracted image stills of higher quality selected for quantitative annotation, revealed only a total of 48 mega-epifauna morphospecies (Table 4), with singletons (morphospecies only observed once)

accounting for 52% of total morphospecies richness. Differences regarding motile morphospecies (decapods, fishes and jellyfish) were also observed between qualitative and quantitative analysis, but these taxa were descriptively analysed separately.

Table 4 –The morphospecies numbers per taxa. The numbers in brackets indicate the number of highly motile morphospecies excluded from the composition and diversity analysis.

PHYLUM	TAXA	Morphospecies richness	
		Qualitative	Quantitative
Annelida	Polychaeta	3 (1)	1
Arthropoda	Pycnogonida	1	1
	Crustacea	9 (5)	6 (4)
Chordata	Tunicata	1	1
	Actinopterygii	(12)	(8)
Ctenophora	Ctenophora indet	(1)	-
Bryozoa	Bryozoa	1	-
Cnidaria	Actiniaria	4	2
	Antipatharia	5	4
	Alcyonacea	7	6
	Pennatulacea	2	1
	Ceriantharia	3	2
	Anthozoa indet	1	1
	Cnidaria indet	(9)	(4)
Echinodermata	Asteroidea	4	2
	Echinoidea	2	2
	Holothuroidea	16 (1)	11
	Ophiuroidea	1	1
Hemichordata	Enteropneusta	1	1
Mollusca	Cephalopoda	1	1
	Scaphopoda	1	1
Porifera	Cladorhizidae	1	-
	Porifera indet	11	4
TOTAL		**79 (29)**	**48 (16)**

Overall, the most frequent taxa observed along the Gloria Fault were Cnidaria and Echinodermata. Specifically, the classes Anthozoa and Holothuroidea were the most common taxa observed, being present at all work areas. In addition, Anthozoa and Holothuroidea also comprised the highest number of morphospecies, with respectively, 16 and 11 morphospecies observed in quantitative analysis and respectively, 22 and 17 morphospecies observed in qualitative analysis. In addition, altogether both represented approximately half of all mega-

epifauna morphospecies observed in both analysis (Table 4). On the contrary, Porifera, Polychaeta, Tunicata, Enteropneusta and Mollusca represented smaller proportions of the mega-epifauna, being less observed and having lower morphospecies richness.

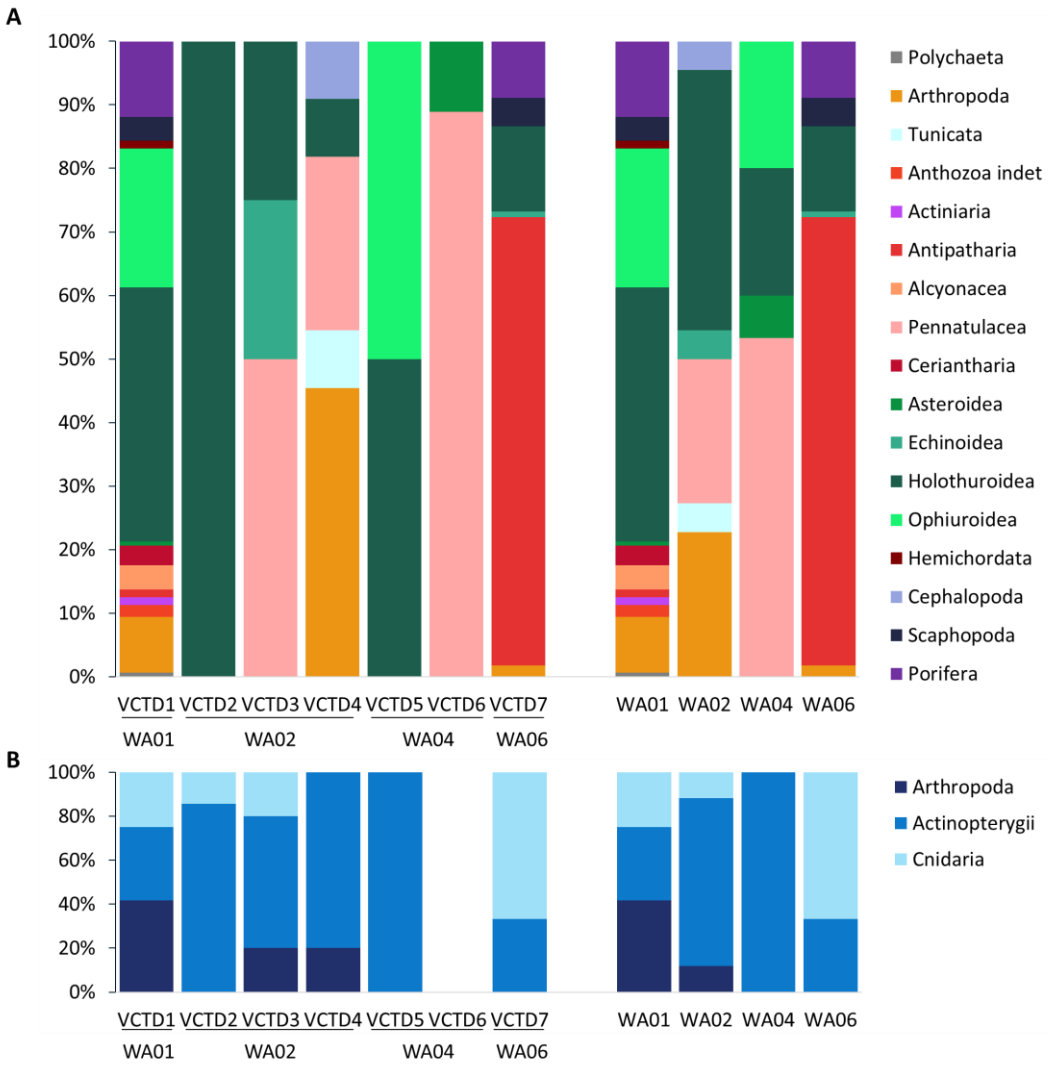

Figure 15 - Relative frequency (%) calculated based on density **(A)** of the main taxonomic groups and **(B)** of the main motile taxa per sampling stations and work areas.

The mega-epifauna and mobile taxa composition within work areas was highly variable (Fig.15A and B). Holothuroidea represented the highest proportions of the total density of Terceira rift and western Gloria (WA01 and WA02, 40 and 41%, respectively). At WA01, the second and third most common groups were Ophiuroidea (22%) and Porifera (12%), while at WA02, it was Arthropoda (23%) and Pennatulacea (23%) (Fig.15A). On the contrary, at central Gloria and eastern Gloria, Holothuroidea represented lower proportions (WA04 and WA06, 20

and 13%, respectively), and the class Anthozoa, precisely Pennatulacea and Antipatharia orders, presented the highest proportions instead (53 and 71%; Fig.15A). At WA04, the second and third most common group was Ophiuroidea (20%) and Holothuroidea (20%), while at WA06 was Holothuroidea (13%) and Porifera (9%; Fig.15A). With regards to the motile taxa composition, Actinopterygii was the most common taxa observed, being present at all work areas (Fig.15B). Nonetheless, variable proportions of Cnidaria and Arthropoda were also observed at WA01, WA02 and WA06, while absent from WA04 (Fig.15B).

The Non-Metric Multidimensional Scaling (nMDS; Fig.16A) showed no clear segregation between images analysed across all sampling stations and work areas, associated to a large variability between observations and sparsely distributed fauna. In agreement, the PERMANOVA did not detect significant differences between work areas (Pseudo-F=1.2506, $p>0.05$; Annex Table A8) and dispersion within work areas was detected by the PERMDISP analyses ($p<0.05$; Annex Table A7). Similarity Percentage Analysis (SIMPER) results revealed an overall low similarity between observations of the same work area, particularly within WA02 and WA01 (9 and 19%), while average dissimilarities between work areas, ranged between 90 and 100% (Table 5). The morphospecies with the highest contributions for both similarity and dissimilarity belonged to the taxa Holothuroidea, Ophiuroidea, Pennatulacea, Arthropoda and Antipatharia, which corresponded to the taxonomic groups also representing the highest proportions at different work areas (Table 5, Fig.15A). When observations were pooled per sampling station, the sampling stations from the work areas of WA02 and WA04 appeared separated from the sampling stations of WA01 and WA06 (Fig 16B).

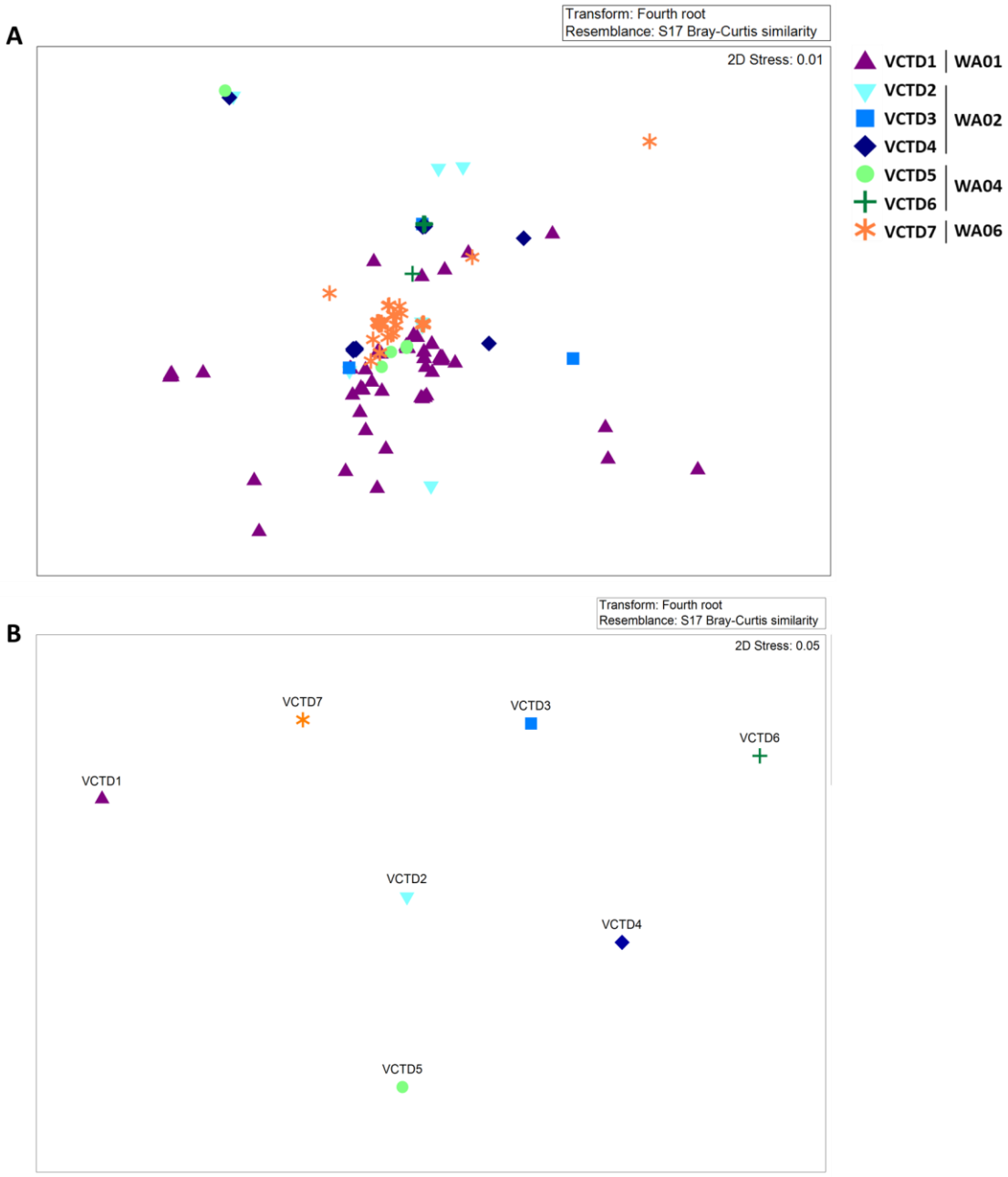

Figure 16 - Non-Metric Multidimensional Scaling (nMDS) displaying **(A)** images with mega-epifaunal observations and **(B)** pooled observations per sampling station.

Table 5 - Breakdown of percentual contributions (%) of morphospecies for similarities and dissimilarities from SIMPER analysis based on single still image as main sampling unit.

		WA01	WA02	WA04	WA06	WA01 and WA02	WA01 and WA04	WA02 and WA04	WA01 and WA06	WA02 and WA06	WA04 and WA06
		Average similarity				Average dissimilarity					
		18.8	9.0	29.4	49.5	99.8	94.8	90.1	99.8	98.7	99.9
Taxa	**Morphospecies code**	% Contribution for similarity				% Contribution for dissimilarity					
Echinodermata		-	-	-	-	-	-	-	-	-	-
Holothuroidea	Hol_013	-	-	-	-	4.4	-	4.9	-	4.0	-
Elpidiidae	Hol_003	57.4	-	-	-	17.4	17.0	-	14.8	-	-
	Hol_004	-	-	-	-	2.5	2.5	-	2.2	-	-
	Hol_006	-	-	-	-	4.6	3.4	8.1	-	4.2	-
	Elpidiidae indet	-	5.0	-	-	5.1	-	4.8	1.1	4.3	-
Psychropotes	Hol_008	-	-	-	-	2.2	-	-	-	-	-
Synallactidae	Hol_010	-	5.2	-	-	4.8	-	5.0	7.7	10.9	7.5
Deimatidae	Hol_012	-	-	-	-	-	6.6	7.4	-	-	6.1
Asteroidea	Asteroidea indet	-	-	-	-	-	3.8	4.3	-	-	3.3
Ophiuroidea	Oph_001	38.7	-	9.3	-	14.0	18.5	11.7	11.9	-	9.0
Echinoidea	Ech_001	-	-	-	-	2.3	-	-	-	2.1	-
Cnidaria		-	-	-	-	-	-	-	-	-	-
Anthozoa	Ant_007	-	-	-	-	-	0.9	-	0.8	-	-
Antipatharia	Ant_008	-	-	-	94.7	-	-	-	37.2	39.9	37.0
Umbellulidae	Pen_001	-	30.0	87.6	-	9.0	28.9	31.9	-	8.2	25.0
Ceriantharia	Cer_001	-	-	-	-	1.8	1.8	-	1.5	-	-
Mollusca		-	-	-	-	-	-	-	-	-	-
Cephalopoda	Mol_001	-	-	-	-	2.2	-	-	-	-	-
Scaphopoda	Mol_002	-	-	-	-	1.9	1.8	-	3.9	2.6	-
Arthropoda		-	-	-	-	-	-	-	-	-	-
Galatheidae	Cru_009	-	50.0	-	-	11.2	-	12.3	-	10.2	-
	Cru_010	-	-	-	-	-	-	-	0.8	-	-
Porifera		-	-	-	-	-	-	-	-	-	-
	Por_001	-	-	-	-	1.0	1.0	-	0.8	-	-
	Por_004	-	-	-	-	-	-	-	4.3	4.6	4.3
	Por_005	-	-	-	-	1.8	1.8	-	1.6	-	-
	Por_012	-	-	-	-	2.4	2.3	-	2.0	-	-
Chordata		-	-	-	-	-	-	-	-	-	-
Tunicata	Tun_001	-	-	-	-	2.2	-	-	-	-	-
% Total contribution of taxa		96.1	90.3	96.9	94.7	90.4	90.3	90.4	90.5	91.1	92.1

3.2.3. Diversity

Overall, the highest mega-epifauna morphospecies richness was observed at the Terceira rift (WA01; 32 morphospecies). Morphospecies richness across the remaining work areas was 3 to 6 times lower (ranging between 5 and 10 morphospecies; Table 6).

Table 6 – Overview of the diversity results based on pooled results per sampling station and work area. Variables measured include total number of individuals (N), morphospecies richness (S), Pielou's Evenness (J'), Shannon-Wiener index (H'), and Hill Numbers (N_1, N_2 and N_∞)).

	S	N	J'	$H'_{(loge)}$	N_1	N_2	$N\infty$
VCTD1	32	160	0.72	2.49	12.09	6.41	3.27
VCTD2	5	7	0.96	1.55	4.71	4.45	3.50
VCTD3	3	4	0.95	1.04	2.83	2.67	2.00
VCTD4	5	11	0.85	1.37	3.92	3.27	2.20
VCTD5	3	6	0.92	1.01	2.75	2.57	2.00
VCTD6	2	9	0.50	0.35	1.42	1.25	1.13
VCTD7	10	112	0.48	1.11	3.03	1.96	1.44
WA01	32	160	0.72	2.49	12.09	6.41	3.27
WA02	10	22	0.92	2.11	8.23	6.91	4.40
WA04	5	15	0.80	1.29	3.62	2.85	1.88
WA06	10	112	0.48	1.11	3.03	1.96	1.44
Total	48	309	0.72	2.80	16.47	8.69	3.96

Overall, across the different diversity indices investigated based on pooled results per work area, the Shannon-Wiener and the Hill Number indices indicated an overall lower diversity and higher morphospecies dominance at WA04 (H'=1.29, N1=3.62; N2=2.85 and N_∞=1.88) and WA06 (H'=1.11, N1=3.03, N2=1.96 and N_∞=1.44), while the WA01 (H'=2.49, N1=12.09, N2=6.41 and N_∞=3.27) and WA02 (H'=2.11; N1=8.23, N2=6.91 and N_∞=4.40), presented higher values (Table 6). In addition, WA06 showed the lowest Pielou's Eveness observed (J'=0.48), also indicating higher dominance by a single species (Table 6). All rarefaction curves showed relatively steep curves (partially explained by the large number of singletons), and did not stabilize/reach an asymptotic value, implying an insufficient amount of observations to capture the totality of morphospecies richness across the Gloria Fault (Fig.17). Particularly, the curves from the work area WA01 and WA02 and respective sampling stations, showed steeper curves by comparison to work areas WA04 and WA06 and respective sampling stations (Fig.17A and B).

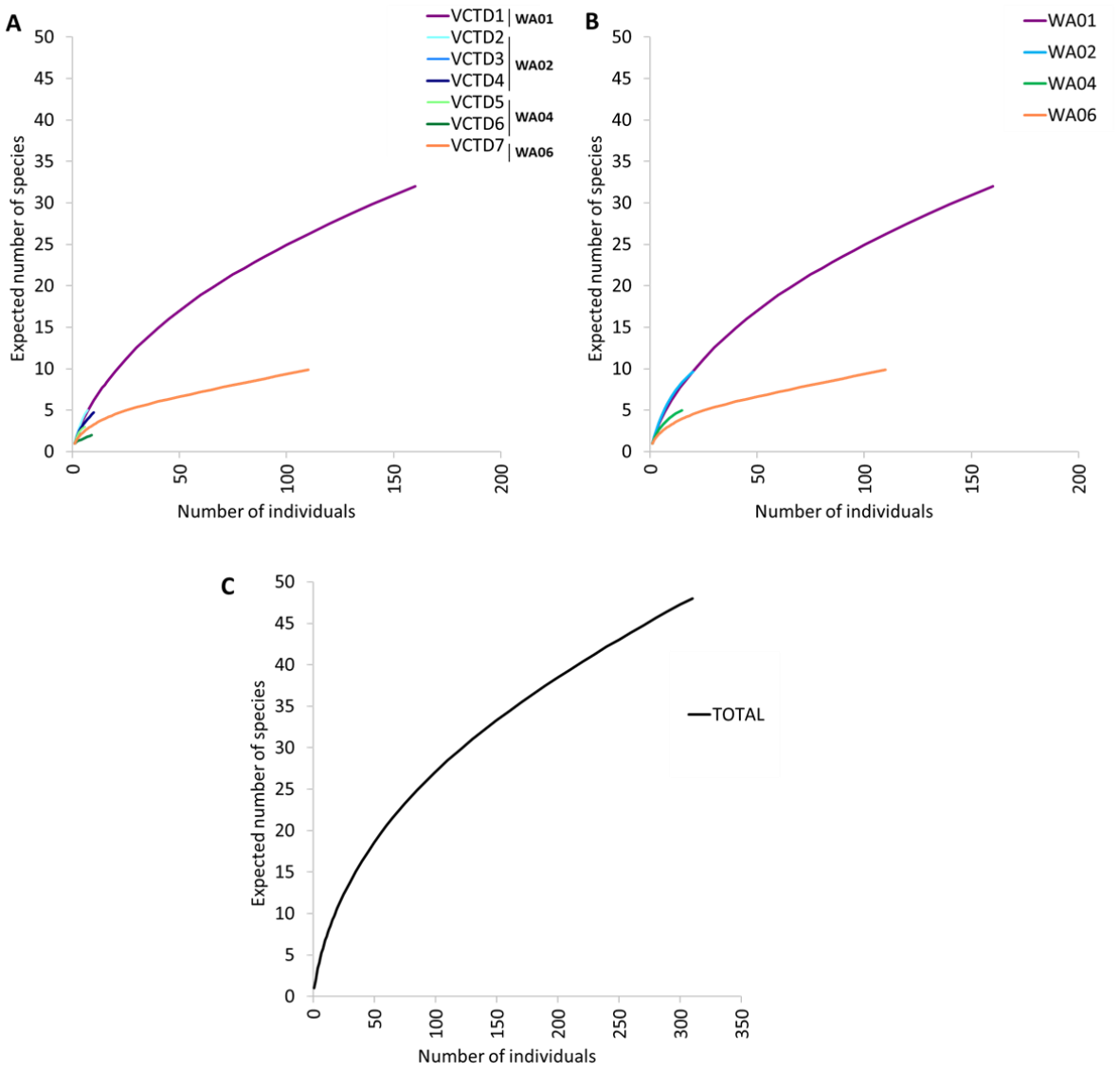

Figure 17 - Comparison of rarefaction curves plotted based on Hurlbert Expected Species Richness (ES(n)) and number of individuals (n) of different **(A)** sampling stations**, (B)** work areas and the **(C)** total for the Gloria Fault.

The partitioning of diversity in alpha and beta diversity components, revealed that most of the diversity, for both species richness and Shannon-Wiener index, relies highly on the component of beta diversity, specifically, within sampling stations (40 and 59%, respectively) and between work areas (56 and 32%, respectively; Fig.18). On the other hand, the alpha diversity (diversity within still images/samples; 3 and 6%, respectively) and the beta diversity between sampling stations (1 and 3%, respectively), represent very small proportions (Fig.18).

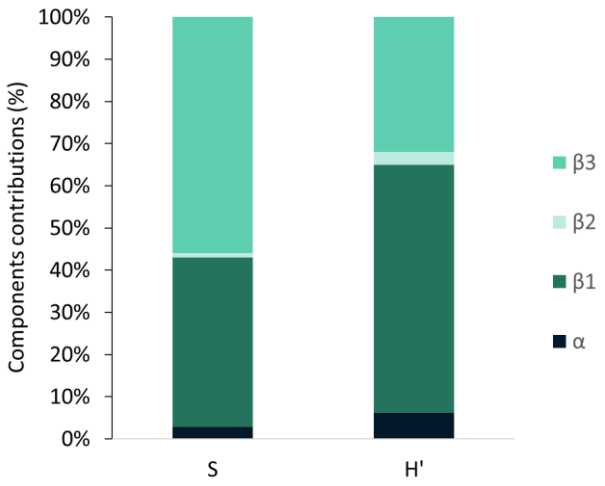

Figure 18 – Diversity component contributions (α, β1, β2 and β3; %) to species richness (S) and Shannon-Wiener diversity index. α: diversity within samples (image stills), β1: β-diversity within sampling stations, β2: β-diversity between sampling stations and β3: β-diversity between areas.

3.2.4. Functional trait composition

Overall, all work areas were mostly composed of variable proportions of both epibenthic and benthopelagic modalities, but at WA01 a higher number of tiering modalities was observed, due to including an infauna morphospecies (Fig.19A). Specifically, the majority of individuals present across work areas, with the exception of WA02, were classified as epibenthic organisms (ranging between 92 and 97%), while benthopelagic (ranging between 3 and 7%) and infauna (ranging between 0 and 1%) organisms were found in much smaller proportions (Fig.19A). At the WA02, similar proportions of both epibenthic (56%) and benthopelagic (44%) organisms were observed instead (Fig.19A).

With regards to motility, sessile and discreetly motile organisms predominated, but all motility modalities investigated were present across the Gloria Fault (Fig.19B). The WA01 presented the highest proportions of discreetly motile organisms (63%) followed by sessile (22%), while the WA06 presented the highest proportions of sessile organisms (77%), followed by discreetly motile (18%; Fig.19B). At WA02, motile organisms were observed with the highest proportions (59%) followed by discreetly motile (26%) and at WA04 similar proportions of both sessile (50%) and discreetly motile organisms (44%) were found (Fig.19B).

In terms of feeding mode, the Gloria Fault composition was highly variable across the work areas, with an overall presence of all modalities investigated along the studied region (Fig.19C). The WA01 was mostly composed of deposit feeders (63%) followed by suspension feeders (21%) (Fig.19C). In contrast, predators (48%) were the main group observed at the

WA02, accompanied by variable proportions of deposit feeders, suspension feeders, predators and scavengers/omnivores (ranging between 12% and 24%) (Fig.19C). The WA04 presented similar proportions of both deposit feeders (44%) and suspension feeders (50%), while the WA06 was dominated by suspension feeders (77%) (Fig.19C).

Noteworthy, general patterns in functional traits composition across work areas were associated with a high variability, due to heterogeneity in functional traits observed between the sampling stations, particularly evident at WA04 (Fig.19).

Figure 19 - Relative frequency (%) calculated based on density of the **(A)** tiering, **(B**) motility and **(C)** feeding mode modalities, per sampling station and work area.

3.3. Relation between mega-epifauna and environmental setting across the Gloria Fault

The Distance-Based Linear Model (DISTLM) revealed that all variables alone (marginal tests, p<0.01; Annex Table A9) were significantly correlated with mega-epifaunal composition across the sampling stations investigated and together explained 28.93% of the total variability observed along the Gloria Fault. The sequential tests identified by order of importance, turbidity (18.3%, p<0.01) followed by salinity (4.5%, p<0.01), SVI (2.1%, p<0.01), water depth (1.3%, p<0.01), NPP (0.9%, p<0.01) and oxygen concentrations (0.6%, p<0.05; Annex Table A9) as main significant contributors.

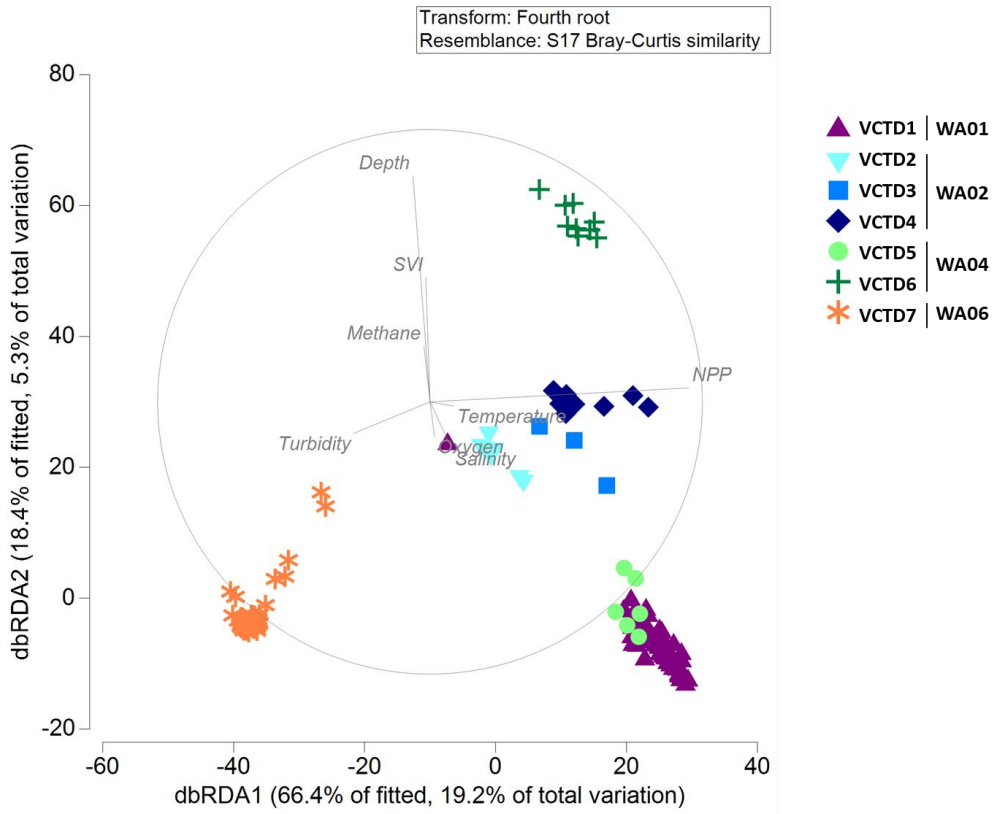

Figure 20 - Distance-Based Redundancy Analysis (dbRDA) plot investigating the relationship between mega-epifauna composition and environmental variables.

The distance-based redundancy (dbRDA) plot explained 24.5% of the total variation and demonstrated that the highest temperatures, oxygen concentrations and NPP poy differentiated the WA01 from the remaining, while the increase in turbidity potentially resulted in the differentiation of WA06 (Fig.20), as shown previously also in the PCA plot showing variation in environmental variables alone (Fig.12). On the other hand, an overall similarity in

the environmental variables, which previously grouped observations from WA02 and WA04 as observed in a PCA plot (Fig.12), was not matched by the dbRDA plot (Fig.20). Specifically, the sampling stations within WA04 are shown separated, possibly due to the very small proportions of the variability explained by the current model (Fig.20).

Regarding the seabed type, it was observed that higher morphospecies richness was observed at the WA01, where a greater number of different types of seabed type including hard substrata was also observed (muddy sediments with basalt outcrops or sparce boulders and basalt walls). Specifically, sessile species represented 50% of the total morphospecies richness at the WA01, while at the remaining work areas the percentage of sessile species only ranged between 20 and 30%.

3.4. *Lebensspuren* (animal traces)

A total of 728 *lebensspuren* traces were registered across this study, with an additional 295 observations of detritus and dead stalks. Overall, density of *lebensspuren* traces increased eastwards, specifically from Terceira rift to eastern Gloria (WA01 to WA06) from 0.98±1.426 to 5.26±4.993 traces.m^{-2}, while the densities at the western and central Gloria (WA02 and WA04) corresponded to 1.33±2.000 and 2.66±4.186 traces.m^{-2}, respectively (Fig.21). The significant PERMDISP results ($p<0.01$; Annex Table A4) suggested high variability within work areas, and therefore no significant differences between work areas could be confidently assigned (Annex Table A5).

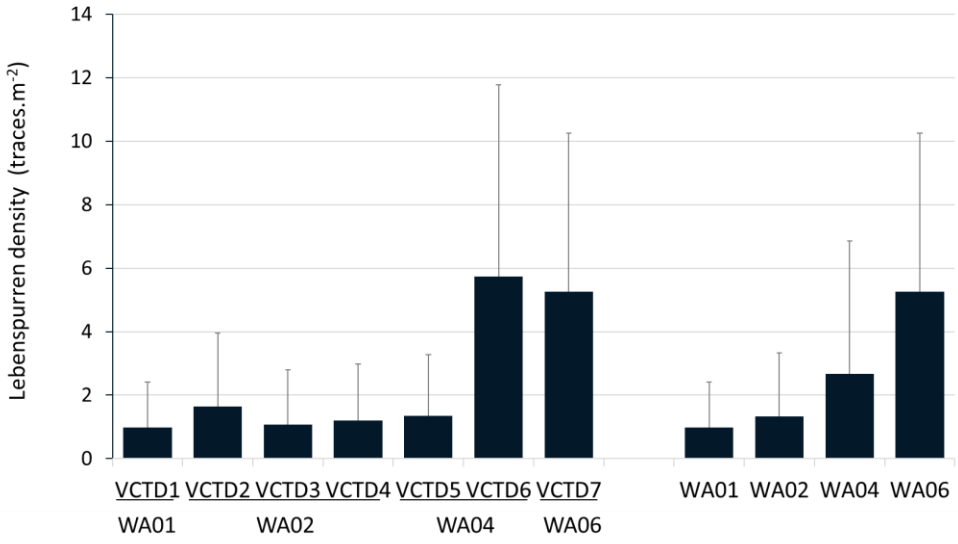

Figure 21 - Average density ± standard deviation of *lebensspuren* (traces.m^{-2}) per sampling station and work area.

Overall, feeding and foraging traces dominated the *lebensspuren* composition across work areas (ranging between 49 and 80%), followed by burrows and mounds (ranging between 14 and 41%), and then locomotion traces (ranging between 6 and 24%; Fig.22). At WA01, high proportions of feeding and foraging traces were observed (57%), followed by locomotion traces (24%), while at WA02 and WA04 were observed the highest proportions of feeding and foraging traces (76 and 80%), followed by burrows and mounds (17 and 14%; Fig.22). The work area WA06 presented the same pattern, but the proportion of feeding and foraging traces (49%) was lower and comparable to burrows and mounds (41%; Fig.22).

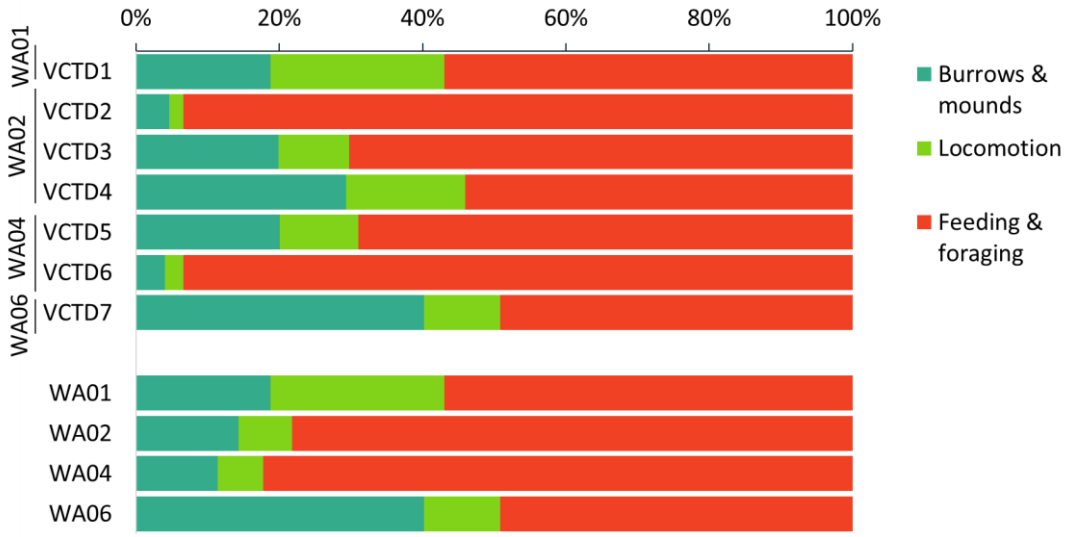

Figure 22 - Relative frequency (%) calculated based on density of different types of traces per sampling station and work area.

Despite overall high proportions of feeding and foraging traces, when exploring the different types of these traces in detail, there was a clear differentiation between work areas. In WA01, the most common traces were the spiral Enteropneusta feeding traces (64%) followed by faecal casts, most likely of holothurians (Fig.23C). On the other hand, Echiura rosette traces were predominant in WA02, WA04 and WA06 (Fig.23C). Faecal casts were also present with relatively higher proportions at WA04 (20%), whereas they were almost absent at WA02 and WA06 (2 and 3%) (Fig.23C). Asteroidea impressions and traces associated to sessile fauna (likely to Antipatharia), were overall the least observed across all areas investigated and were only respectively present at two (WA02 and WA04, 1 and 3%, respectively) and one work area (WA06, 3%) (Fig.23C).

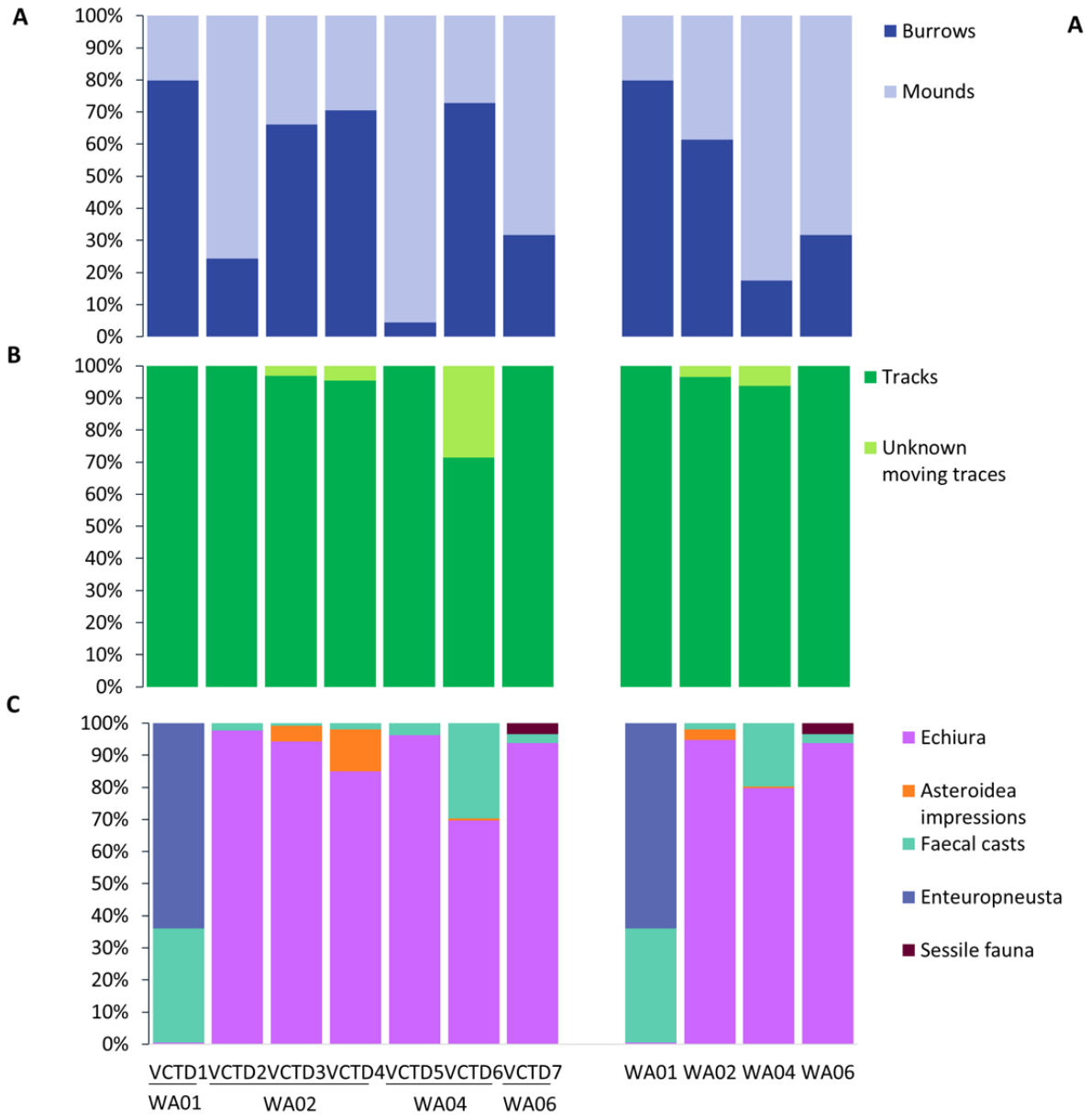

Figure 23 - Relative frequency (%) calculated based on density of **(A)** burrows and mounds, **(B)** locomotion traces and **(C)** feeding and foraging traces.

With regards to the locomotion traces, most traces were composed of tracks, likely of holothurians or echinoids, but also an unknown moving trace observed in higher proportions WA02 an WA04 (Fig.23B). In terms of burrows and mounds, burrows respectively presented higher proportions in WA01 and WA02, while mounds were observed in higher proportions at WA04 and WA06 (Fig.23A).

3.5. Evidence of anthropogenic disturbance by marine litter

A total of 52 litter items were observed across the surveyed seabed, exclusively at muddy sediments. Most items were composed by plastic (71-90%), but metal (0-17%), glass (0-10%) or lost fishing gear (0-13%) items were also found in smaller proportions (Fig.24). In addition, 12% of the total items observed were either entangled or associated in some form to mega-epifaunal organisms (Annex Fig.1A).

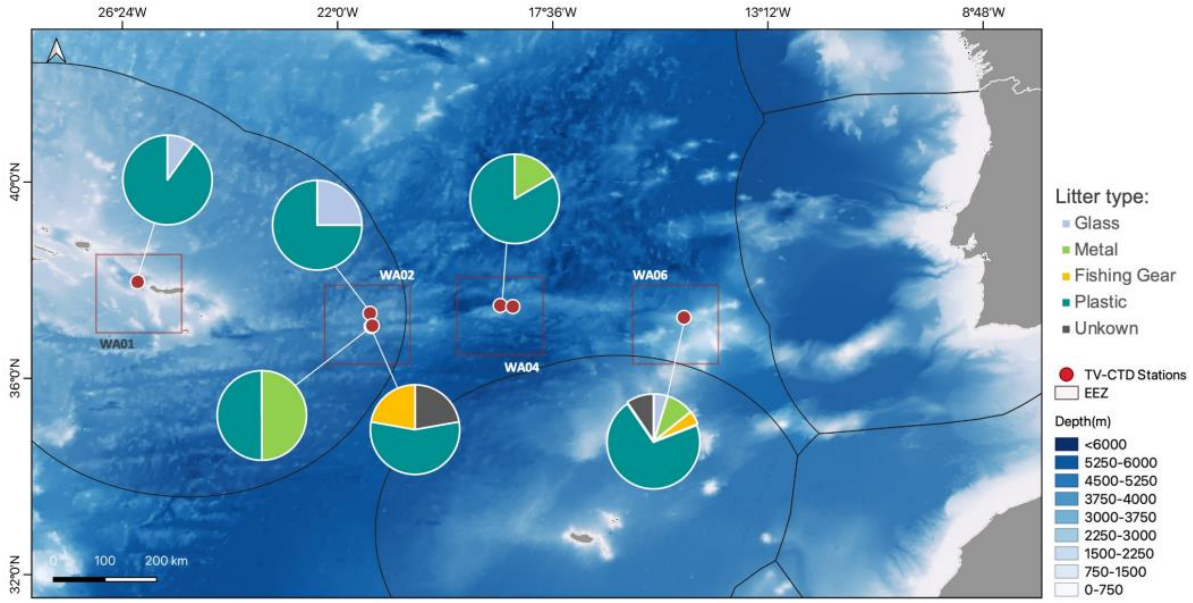

Figure 24 - Relative frequency (%) calculated based on density of different marine litter types per sampling station and work area.

Overall, litter was observed at all work areas. However, at the sampling station VCTD5 located within the WA04 litter was not observed (Fig.25). The average density observed per work area increased eastwards from WA01 to WA06, ranging from 0.02±0.147 to 0.14±0.640 items.m^{-2}. Between sampling stations within the WA02, the density was similar across sampling stations (ranging from 0.01±0.043 and 0.03±0.147 items.m^{-2}; Fig.25), but within the WA04, litter wasn't observed at the sampling station VCTD5, while at VCTD6 the litter density was one of the highest (0.11±0.501 items.m^{-2}; Fig.25). Across sampling stations specifically, the densities were on average about 9 times higher at VCTD6 and VCTD7/WA06 by comparison with the remaining (Fig.25).

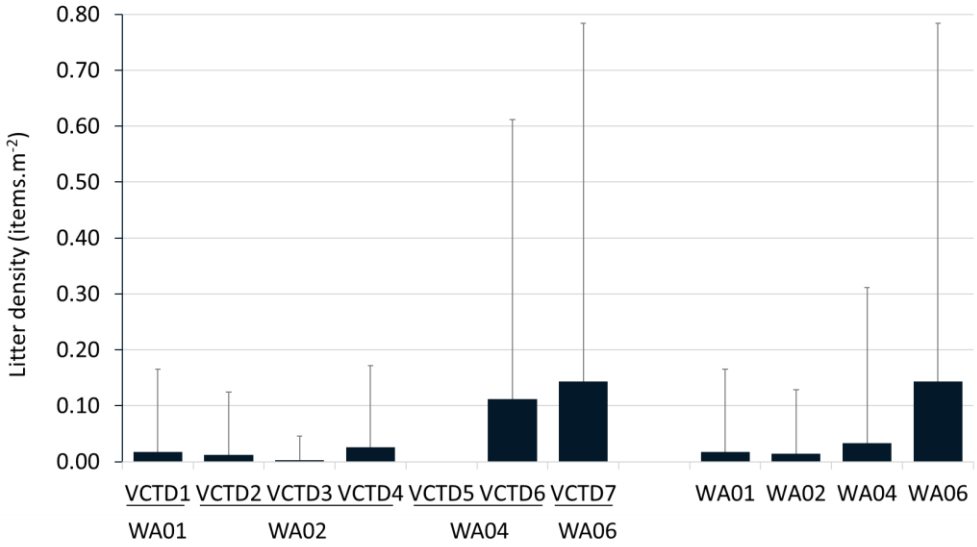

Figure 25 – Average density ± standard deviation of litter (items.m^{-2}) per sampling station and work area.

4. DISCUSSION

4.1. Environmental setting variation

Fracture zones and associated faults represent areas of potentially heterogenous environmental settings due to complex geomorphology and potentially associated chemosynthetic conditions. The environmental variation observed across the four work areas surveyed in this study reflects a bathymetric variation within abyssal ranges across the Gloria Fault, ranging between 3185 and 4665 m. This variation showcases the outcomes of prominent geomorphological expression of the Gloria Fault (Omira et al., 2019). In addition to bathymetric variation, seabed heterogeinity was also evidenced through the visual assessment of the seabed, by the observation of steep vertical walls covered in sediments or evidence of basalts and other hard substrata in between large extensions of muddy sedimented areas.

The depth differences across the Gloria Fault, together with the potential influence of the Azores at west and of the Madeira Tore Rise at east, could help explain the overall variation of environmental variables across the different work areas. A smaller variation in the environmental variables was observed across the deepest studied areas, located respectively in the western and central Gloria (WA02 and WA04) and characterised by the lowest temperatures, oxygen concentrations and turbidity. On the other hand, the conditions observed at the Terceira rift and eastern Gloria near the Madeira Tore Rise (WA01 and WA06) presented variations. Specifically, higher temperatures and oxygen concentrations characterised the

Terceira rift in proximity to the Azores (WA01), located at the shallowest depths, while the lower methane concentrations and higher turbidity, characterised the eastern Gloria in proximity to the Madeira Tore Rise complex (WA06). Noteworthy, all the reported temperatures, oxygen concentrations and salinity fell into ranges previously reported for the predominant water masses that influence the Gloria Fault region (i.e, temperatures between 1.95- 3.33 ºC; oxygen concentrations between 245-280 µmol.l^{-1} and constant salinity of 35), with deviations occurring only at the Terceira rift in proximity to the Azores region, due to presenting higher temperatures and oxygen concentrations (Liu and Tanhua, 2021). The surface conditions relating to primary productivity did not seem to follow the same pattern as the remaining variables, apart from the fact that Terceira rift presented a higher primary productivity and associated seasonal variation. The differences in higher surface productivity and higher seasonal variation at the Terceira rift, could be explained by the influence of the Azores, which has been discussed as a major atmospheric carbon sink, due to the amount of primary production taking place there, especially during the spring enrichment traced to the Gulf Stream (Caldeira and Reis, 2017). This can be directly associated to the higher levels of primary productivity evidenced and in addition explain the higher seasonal variation observed, due to biological enrichment seasonality (Caldeira and Reis, 2017). With regards to the higher turbidity levels observed at the easternmost site, the influence of the Madeira Tore Rise complex as a result of comprising various seafloor elevations, as well as the influence of the formation of meddies (Serra and Ambar, 2002) could possibly justify the highest levels of turbidity, due to modified currents and near bottom flows (Lavelle and Mohn, 2010).

4.2. Mega-epifaunal variation

In the present study, no significant differences across the abyssal areas surveyed could be accurately detected, both in terms of total density and composition of mega-epifauna. This was due to a high variability observed across observations, associated with the sparse distribution of the mega-epifauna along the Gloria Fault. Nonetheless, generally the lowest densities were typically observed at the deepest areas located at western and central Gloria (WA02 and WA04), while the highest densities were observed at the eastern Gloria and at the Terceira rift (WA06 and WA01) characterised by the shallowest depths. The densities observed across the work areas fell within the ranges reported for the North Atlantic (Thurston et al., 1994, 1998; Durden et al., 2015; Bell et al., 2016; Alt et al., 2019). Specifically, only the values from the Terceira rift (WA01) fell within the ranges of the Porcupine Abyssal Plain, determined at abyssal hills and plains (Durden et al., 2015), while all values were higher than those reported at Madeira Abyssal Plain (Thurston et al., 1994, 1998). However, the values determined at the Madeira Abyssal Plain could be associated to the differences between

sampling methods, due to the fact that in Thurston et al (1994) and (1998) epibenthic sledges and otter trawls were used instead, possibly bringing problems to density estimation (e.g. the abundances determined in imagery were higher). The values reported for the Charlie Gibbs Fracture Zone were the ones most effectively capturing the range of values observed across the Gloria Fault (Alt et al., 2019; Bell et al., 2016). In addition, variation in density observed over a large time period at station M, comprised most values recorded at the present study, only with exception of the lowest value, possibly indicating that the observed densities at the present study are not abnormal when temporal variation is considered (Kuhnz et al., 2020).

Regarding the composition at high taxa, the differences observed between work areas were generally associated with a high variability in proportions of the predominant and most common taxa: Anthozoa and Holothuroidea. The taxa Holothuroidea predominated at Terceira rift (WA01) and western Gloria (WA02). By opposition, Anthozoa presented high proportions at central and eastern Gloria (respectively, the orders Pennatulacea and Antipatharia). The predominant presence of Echinodermata at the Terceira rift and western Gloria (WA01 and WA02) goes in agreement with was previously observed across the North Atlantic, namely at the Porcupine Abyssal Plain (Thurston et al., 1994, 1998) and at some sites across the Charlie-Gibbs Fracture Zone (Alt et al., 2019). In addition, high proportions of echinoderms, namely Holothuroidea, are generally observed below 2000 m by comparison with other taxa (Gebruk et al., 2010). By opposition, at the Madeira Abyssal Plain, natant Decapoda and Asteroidea (Thurston et al., 1998), and in addition Bivalvia (Thurston et al., 1994) were amongst the most abundant taxa, differing with was observed across Gloria Fault. The high proportions of Anthozoans observed in central Gloria and eastern Gloria (WA04 and WA06), might represent a distinction to what was previously mostly observed in the previously mentioned studies. Nevertheless, species with wide distributions of Anthozoa orders, including of Pennatulacea and Antipatharia, have been previously assessed and recorded across the northern Mid Atlantic Ridge and Charlie Gibbs Fracture Zone (Molodtsova et al., 2008).

Considering morphospecies richness along the Gloria Fault, a lower total number of morphospecies was observed at the present study by comparison with the ranges reported across Charlie Gibbs Fracture Zone (Alt et al., 2019; Bell et al., 2016), but comparable to the total number observed at abyssal depths in Porcupine Abyssal Plain (43 morphospecies) (Durden et al., 2015), even though the present study counted with a larger scale setting. With regards to spatial variation in diversity, similarly to what was observed across the Charlie Gibbs Fracture Zone, differences in diversity were also observed between areas located at different sites (Alt et al., 2019). Considering the variation of individuals proportion across morphospecies, indices highlight that Terceira rift and western Gloria (WA01 and WA02) are

the most diverse, while the central and eastern Gloria (WA04 and WA06) the least, pointing out that the structure of mega-epifauna at these work areas is less equitable. These results indicate a different pattern in diversity from density, as the two areas with the highest densities (WA01 and WA06) presented contrasting levels of diversity. By comparison with the Charlie Gibbs Fracture Zone, where overall high levels of evenness were observed (J': 0.93–1.00), only the values of western Gloria work area were comparable (Bell et al., 2016), while by comparison with Porcupine Abyssal Plain the evenness varied between lower values than those observed at the Gloria Fault (J': 0.07-0.11; Durden et al., 2015). The diversity partitioning revealed that the major portion of diversity was associated to diversity within sampling stations, followed by diversity between work areas, highlighting the large variability in morphospecies presence and a high number of singletons/rare taxa spatially distributed across the Gloria Fault, in agreement with most observations done in abyssal regions of the world (Ebbe et al.,2010).

4.3. Relation between mega-epifauna and environmental setting

Generally, a reflection of environmental setting differences in mega-epifauna parameters was observed. Specifically, the lowest densities observed in the study were from the deepest work areas at western and central Gloria (WA02 and WA04). The results could be in major part explained by the depletion of food availability with increasing depth, known to be a key structuring variable in deep sea benthic standing stocks but also diversity (Rex, 1981; Rex et al., 2006). In addition, the results also agree with the expectation that changes in distance from continental margins comprising changes in POC flux, with higher quantity and quality found near coastal zones, can be reflected in mega-epifaunal parameters (Levin et al., 2001; Smith et al., 2008). In this case, the presence of the Azores as a landform could be associated with higher quantities and quality of POC flux, which increase the food availability at Terceira rift (WA01) and hence the high mega-epifaunal density. Furthermore, the differences observed in the present study could reflect similar differences to those reported across a landscape variation and bathymetric variation (3950-4250 m), revealing that more elevated places, were associated with higher densities overall (Simon-Llédo et al., 2019).

With regards to diversity, the Terceira rift (WA01) was one of the most diverse areas. The higher presence of hard substrata creating an interruption of the soft sediments at the Terceira rift (WA01) possibly contributed to the high diversity in this location, as it is observed that the presence of hard substrate promotes the presence of sessile taxa such as corals and sponges, which would otherwise be present in very low abundances or not at all (e.g. Vanreusel et al., 2016). For example, although at much lower depths, dropstones which

constituted very low proportions of the total seafloor area surveyed, were associated to 20% of the overall species richness reported by Ziegler et al. (2017). In agreement, although hard substrata was present in low proportions at the Terceira rift, the sessile species visibly attached to hard substrata represented 50% of the total morphospecies richness. In addition, higher species richness across the Charlie Gibbs Fracture Zone was previously observed in transects where an intermediate substratum coverage of rock was also observed (Bell et al., 2016). This is verified only for diversity and not for density, perhaps due to the fact that the hard substrata presence was sparse and not very abundant, hence not allowing the substantially abundant settlement of sessile taxa.

The presence of sessile and suspension feeders by association across the Gloria Fault could be associated to other factors, besides only the availability of visible hard substrata. In association to the eastern Gloria (WA06), it is verified that the presence of sessile and suspension feeders' taxa does not affect the diversity of the area, as this site presented one of the less equitable assemblages' structures and is dominated by density by a single sessile Antipatharian. Nevertheless, in this case this sessile morphospecies wasn't found visibly attached to hard substrata, suggesting that the factor influencing its presence might be the influence of Madeira Tore complex seamounts and intensified near-bottom currents, possibly also associated to the higher turbidity observed in the area. The pattern exhibited by the dbRDA and DISTLM results confirmed a pattern of variation regarding mega-epifauna assemblage structure which aligns to a certain degree with the environmental variability and it specifically reinforces that turbidity might have presented a major influence in driving the differences observed at eastern Gloria (WA06). In addition, a small-scale variation in elevation consequently possibly associated to process of modification of currents and near bottom flows, which influence food availability, could also be at stake (Durden et al., 2015; Durden et al., 2020b).

4.4. *Lebensspuren* (animal traces)

The assessment of animal traces provides a long-term information on the presence of different fauna at abyssal benthic environments. In this study, the density of traces increased eastwards resulting in higher densities at eastern Gloria (WA06), where a higher density of mega-epifauna was also observed, similarly to a positive relationship between both the traces and faunal density reported by Bell et al. (2013). By opposition, the Terceira rift (WA01), with the second highest mega-epifauna density, had the lowest traces density.

The feeding and foraging traces presented a wider variety of trace types in terms of composition, including traces which could be more precisely traced to the taxa to which they

were associated. The Terceira rift (WA01) presented contrasting compositions by comparison with other work areas, with high proportions of Enteropneusta traces, which have previously been found in high proportions at bathyal depths across the Charlie Gibbs Fracture Zone (Bell et al., 2013). The Enteropneusta traces were followed by faecal casts (most likely of holothurians), possibly associated to higher abundances of holothurians, as verified before (Bell et al., 2013). On the other hand, the remaining work areas presented similar feeding and foraging traces compositions, where mostly Echiuran traces predominated, which in contrast were previously observed in low proportions at the Charlie Gibbs Fracture zone (Bell et al., 2013). Nevertheless, locomotion traces (highly represented by tracks of echinoderms) did not present high proportions across the present study, although tracks have been previously identified as abundant by Bell et al., (2013).

The presence of Enteropneusta traces dominating the composition of feeding and foraging traces at Terceira rift (WA01) contrasted with low proportions of the organism itself in the imagery annotations and the same was also previously verified (Bell et al., 2013). With regards to Echiuran traces, the proportions contrasted with the no observations of the organism at all work areas. Although in lower proportions, Asteroidea impressions were also observed at western Gloria (WA02), when absence of the organism was also verified. On the other hand, faecal casts, likely of holothurians, were found at all work areas with variable proportions, indicating the widespread presence of the organism.

4.5. Marine litter

Marine litter has been found across all depths, including at remote locations far from shore, with plastic being the most prevalent (e.g., Pham et al., 2014). This goes in agreement with what was observed in the present study, as plastics composed the majority of litter observed and litter was found across all work areas and different corresponding depths. Despite the closeness of the Terceira rift (WA01) to a populated area (the Azores), higher litter densities were not found at this site. On the contrary, a higher variety of types of litter, as well as the highest density, was observed at eastern Gloria in proximity to the Madeira Tore Rise (WA06), highlighting this area as a depositional site, possibly reflecting the influence of the marine traffic and fishing activities in the region, as previously highlighted by Vieira et al., (2015). Nevertheless, Vieira et al. (2015) reported high proportion of fishing gear by comparison to plastic, whereas in the present study there was a predominance of plastic instead, most likely because the study area is further located from the main fishing grounds of the Madeira-Tore seamount complex (Campos et al., 2019).

4.6. Limitations and future perspectives

This study is the first to report on the presence of mega-epifauna along the Gloria Fault. The main limitation of the present study requiring attention in the future, concerns the small number of areas investigated (4 in total) and resultant small surveyed area, along a total extension of approximately 1000 km. In addition, the present study originated from exploratory dives, which limited image quality and resolution of our observations of organisms with size greater than approximately 5cm. Taking upon this, it is important in the future to survey the Gloria Fault with sampling equipment (e.g., high resolution towed cameras systems) and dedicated sampling designs that would allow us to better grasp the spatial variation and diversity across this region. In fact, the requirement for further sampling is supported by the results obtained from the rarefaction curves, which did not reach asymptotic values. Included in this future sampling should also be physical sampling of specimens to confidently identify the taxa observed, particularly within groups in which identification fully relies on physical specimens (e.g., Porifera, Anthozoans). For example, despite the distance between the two deepest areas surveyed at western and central Gloria, a Pennatulacea morphospecies was encountered across both areas. Physical sampling of specimens from both locations would help understand if this morphospecies does have a widespread distribution or if in truth there is two different morphospecies. These perspectives would allow the more precise identifications and quantification of taxa observed. In addition, more extensive sampling would be helpful in capturing the high variability within areas and would allow to better capture the rare morphospecies missed by the current quantitative analysis, as the observed number of morphospecies in a qualitative assessment using all recordings, distinguished a higher number of morphospecies across taxa than the quantitative analysis.

4.7. Conclusion

This study addressed the gap in knowledge regarding abyssal mega-epifaunal assemblages along the Gloria Fault, providing evidence of variation in the main mega-epifauna metrics investigated (e.g., density, composition, diversity) associated to a large-scale variation in the environmental setting. The proposed hypothesis of the present study predicted that the differences observed in terms of environmental conditions between the main areas surveyed would be reflected in density, composition and diversity of mega-epifauna. The central and western Gloria showed similarity in terms of environmental variables, matched by similarity in average mega-epifaunal densities. Nevertheless, in terms of composition and diversity, the same was not clear for these two areas. On the other hand, environmental variation, namely in terms of substrata, turbidity and productivity at Terceira rift and the eastern Gloria, seemed to explain the variation in density, composition and diversity at these locations. Noteworthy,

this study also provided unique knowledge of abyssal mega-epifauna associated with the Gloria Fault, possibly with future relevance for management and conservation actions taken in areas that in a near future will potentially be included within the Portuguese proposal for extension of the continental shelf, currently under evaluation by the United Nations.

REFERENCES

Aller, J. Y. (1989). Quantifying sediment disturbance by bottom currents and its effect on benthic communities in a deep-sea western boundary zone. Deep Sea Research Part A. Oceanographic Research Paper, 36(6), 901-934. DOI: 10.1016/0198-0149(89)90035-6

Alt, C. H., Kremenetskaia, A., Gebruk, A. V., Gooday, A. J., and Jones, D. O. (2019). Bathyal benthic megafauna from the Mid-Atlantic Ridge in the region of the Charlie-Gibbs Fracture Zone based on remotely operated vehicle observations. Deep Sea Research Part I: Oceanographic Research Papers, 145, 1-12. DOI: 10.1016/j.dsr.2018.12.006

Anderson, M. J., Gorley R. N., and Clarke R. K. (2008). Permanova+ for Primer: Guide to Software and Statistical Methods. PRIMER-E Ltd.

Armstrong, C. W., Foley, N. S., Tinch, R., and van den Hove, S. (2012). Services from the deep: Steps towards valuation of deep-sea goods and services. Ecosystem Services, 2, 2–13. DOI: 10.1016/j.ecoser.2012.07.001

Åström, E. K., Carroll, M. L., Ambrose Jr, W. G., Sen, A., Silyakova, A., and Carroll, J. (2018). Methane cold seeps as biological oases in the high-Arctic deep sea. Limnology and Oceanography, 63(S1), 209-231. DOI: 10.1002/lno.10732

Barton, E. D. (2001). Canary and Portugal Currents. In J. H. Stelle, S. A. Thorpe, and K. Turekian, (Eds.), Encyclopedia of Ocean Sciences (pp. 380–389). Elsevier. DOI:10.1006/rwos.2001.0360

Batista, L., Hübscher, C., Terrinha, P., Matias, L., Afilhado, A., and Lüdmann, T. (2017). Crustal structure of the Eurasia-Africa plate boundary across the Gloria Fault, North Atlantic Ocean. Geophysical Journal International, 209(2), 713–729. DOI: 10.1093/gji/ggx050

Behrenfeld, M. J., and Falkowski, P. G. (1997). Photosynthetic rates derived from satellite-based chlorophyll concentration. Limnology and Oceanography, 42(1), 1-20. DOI: 10.4319/lo.1997.42.1.0001

Bell, J. B., Alt, C. H., and Jones, D. O. (2016). Benthic megafauna on steep slopes at the Northern Mid-Atlantic Ridge. Marine Ecology, 37(6), 1290-1302. DOI: 10.1111/maec.12319

Bell, J. B., Jones, D. O., and Alt, C. H. (2013). Lebensspuren of the Bathyal Mid-Atlantic Ridge. Deep Sea Research Part II: Topical Studies in Oceanography, 98, 341-351. DOI: 10.1016/j.dsr2.2012.09.004

Bett, B. J., Malzone, M. G., Narayanaswamy, B. E., and Wigham, B. D. (2001). Temporal variability in phytodetritus and megabenthic activity at the seabed in the deep northeast Atlantic. Progress in Oceanography, 50(1–4), 349–368. DOI: 10.1016/S0079-6611(01)00066- 0

Bett, B. J. (2003). Time-lapse photography in the deep sea. Underwater Technology, 25(3), 121-128. DOI: 10.3723/175605403783379741

Bett, B.J. and Rice, A.L. (1993) The feeding behaviour of an abyssal echiuran revealed by in situ time-Iapse photography. Deep-Sea Research Part I: Oceanographic Research Papers, 40, 1767-1779. DOI: 10.1016/0967-0637(93)90031-W

Billett, D. S. M., Bett, B. J., Reid, W. D. K., Boorman, B., and Priede, I. G. (2010). Long-term change in the abyssal NE Atlantic: The 'Amperima Event' revisited. Deep Sea Research Part II: Topical Studies in Oceanography, 57(15), 1406-1417. DOI: 10.1016/j.dsr2.2009.02.001

Billett, D. S. M., Bett, B. J., Rice, A. L., Thurston, M. H., Galéron, J., Sibuet, M., and Wolff, G. A. (2001). Long-term change in the megabenthos of the Porcupine Abyssal Plain (NE Atlantic). Progress in Oceanography, 50(1–4), 325–348. DOI: 10.1016/S00796611(01)00060-X

Billett, D.S.M., Lampitt, R.S., Rice, AL. and Mantoura, R.F.C. (1983). Seasonal sedimentation of phytoplankton to the deep-sea benthos. Nature, 302, 520-522. DOI: 10.1038/302520a0

Brandt, A., Ellingsen, K. E., Brix, S., Brökeland, W., and Malyutina, M. (2005). Southern Ocean deep-sea isopod species richness (Crustacea, Malacostraca): influences of depth, latitude and longitude. Polar Biology, 28, 284-289. DOI: 10.1007/s00300-004-0688-z

Brandt, A., Linse, K., and Schüller, M. (2009). Bathymetric distribution patterns of Southern Ocean macrofaunal taxa: Bivalvia, Gastropoda, Isopoda and Polychaeta. Deep Sea Research Part I: Oceanographic Research Porcupine Abyssal Plainers, 56(11), 2013-2025. DOI: 10.1016/j.dsr.2009.06.007

Buhl-Mortensen, L., Vanreusel, A., Gooday, A. J., Levin, L. A., Priede, I. G., Buhl-Mortensen, P., Gheerardyn, H., King, N. J., and Raes, M. (2010). Biological structures as a source of tiering heterogeneity and biodiversity on the deep ocean margins. Marine Ecology, 31(1), 21–50. DOI: 10.1111/j.1439-0485.2010.00359.x

Caldeira, R. M. A., and Reis, J. C. (2017). The Azores confluence zone. Frontiers in Marine Science, 4, 1–14. DOI: 10.3389/fmars.2017.00037

Campos, A., Lopes, P., Fonseca, P., Figueiredo, I., Henriques, V., Gouveia, N., Delgado, J., Gouveia, L., Amorim, A., Araujo, G., Drago, T., and dos Santos, A. (2019). Portuguese fisheries in seamounts of Madeira-Tore (NE Atlantic). Marine Policy, 99, 50–57. DOI: 10.1016/j.marpol.2018.10.005

Chapman, A. S., Beaulieu, S. E., Colaço, A., Gebruk, A. V., Hilario, A., Kihara, T. C., Bates, A. E. (2019). sFDvent: A global trait database for deep-sea hydrothermal-vent fauna. Global Ecology and Biogeography, 28(11), 1538-1551.DOI: 10.1111/geb.12975

Chiba, S., Saito, H., Fletcher, R., Yogi, T., Kayo, M., Miyagi, S., Ogido, M. and Fujikura, K. (2018). Human footprint in the abyss: 30 year records of deep-sea plastic debris. Marine Policy, 96, 204-212. DOI: 10.1016/j.marpol.2018.03.022

Clark, M. R., Althaus, F., Schlacher, T. A., Williams, A., Bowden, D. A., and Rowden, A. A. (2016b). The impacts of deep-sea fisheries on benthic communities: a review. ICES Journal of Marine Science, 73, i51-i69. DOI: 10.1093/icesjms/fsv123

Clark, M. R., Consalvey, M., and Rowden, A. A. (2016a). Biological sampling in the deep sea. John Wiley and Sons. DOI:10.1002/9781118332535

Clarke, K. R., and Gorley, R. N. (2015). Getting started with PRIMER v7. PRIMER-E Ltd.

Connolly, T. P., McGill, P. R., Henthorn, R. G., Burrier, D. A., and Michaud, C. (2020). Near-bottom currents at Station M in the abyssal Northeast Pacific. Deep Sea Research Part II: Topical Studies in Oceanography, 173, 104743. DOI: 10.1016/j.dsr2.2020.104743

Cosson-Sarradin, N., Sibuet, M., Paterson, G. L. J., and Vangriesheim, A. (1998). Polychaete diversity at tropical Atlantic deep-sea sites: environmental effects. Marine Ecology Progress Series, 165, 173-185. DOI: 10.3354/meps165173

Costello, M. J., Claus, S., Dekeyzer, S., Vandepitte, L., Tuama, É. Ó., Lear, D., and Tyler-Walters, H. (2015). Biological and ecological traits of marine species. PeerJ, 3, e1201. DOI: 10.7717/peerj.1201

Crist, T. O., Veech, J. A., Gering, J. C., and Summerville, K. S. (2003). Partitioning species diversity across landscapes and regions: a hierarchical analysis of α, β, and γ diversity. The American Naturalist, 162(6), 734-743. DOI: 10.1086/378901

Cuvelier, D., Ribeiro, P. A., Ramalho, S. P., Kersken, D., Martinez Arbizu, P., and Colaço, A. (2020). Are seamounts refuge areas for fauna from polymetallic nodule fields?. Biogeosciences, 17(9), 2657-2680. DOI: 10.5194/bg-17-2657-2020

Danovaro, R., Snelgrove, P. V. R., and Tyler, P. (2014). Challenging the paradigms of deep-sea ecology. Trends in Ecology and Evolution, 29(8), 465–475. DOI: 10.1016/j.tree.2014.06.002

Durden, J. M., Bett, B. J., and Ruhl, H. A. (2020b). Subtle variation in abyssal terrain induces significant change in benthic megafauna abundance, diversity, and community structure. Progress in Oceanography, 186, 102395. DOI: 10.1016/j.pocean.2020.102395

Durden, J. M., Bett, B. J., Huffard, C. L., Pebody, C., Ruhl, H. A., and Smith, K. L. (2020a). Response of deep-sea deposit-feeders to detrital inputs: A comparison of two abyssal time-series sites. Deep-Sea Research Part II: Topical Studies in Oceanography, 173, 104677. DOI: 10.1016/j.dsr2.2019.104677

Durden, J. M., Bett, B. J., Jones, D. O. B., Huvenne, V. A. I., and Ruhl, H. A. (2015). Abyssal hills - hidden source of increased tiering heterogeneity, benthic megafauna biomass and diversity in the deep sea. Progress in Oceanography, 137, 209–218. DOI: 10.1016/j.pocean.2015.06.006

Ebbe, B., Billett, D. S., Brandt, A., Ellingsen, K., Glover, A., Keller, S., Malyutina, M., Arbizu, P. M., Molodtsova, T., Rex, M., Smith, C. and Tselepides, A. (2010). Diversity of abyssal marine life. In McIntyre A. D. (Ed.), Life in the World's Oceans: Diversity, Distribution, and Abundance (pp. 139-160). Wiley. DOI: DOI:10.1002/9781444325508

Emery, W. J. (2001). Water types and water masses. In J. H. Stelle, S. A. Thorpe, and K. Turekian (Eds.), Encyclopedia of Ocean Sciences (pp. 380–389). Elsevier. DOI: 10.1006/rwos.2001.0108

Etter, W., and Hess, H. (2015). Reviews and syntheses: the first records of deep-sea fauna–a correction and discussion. Biogeosciences, 12(21), 6453-6462. DOI: 10.5194/bg-12-6453-2015

Ewing, M., and Davis, R. A. (1967). Lebensspuren photographed on the ocean floor. In J. B. Hersey (Ed.) Deep-sea photography (pp. 259-294) The John Hopkins Press: Baltimore.

Felley, J. D., Vecchione, M., and Wilson Jr, R. R. (2008). Small-scale distribution of deep-sea demersal nekton and other megafauna in the Charlie-Gibbs Fracture Zone of the Mid-Atlantic Ridge. Deep Sea Research Part II: Topical Studies in Oceanography, 55(1-2), 153-160. DOI: 10.1016/j.dsr2.2007.09.021

Forbes, E. (1844) Report on the Mollusca and Radiata of the Aegean Sea, and on their distribution, considered as bearing on geology. Report of the British Association for the Advancement of Science for 1843 (pp. 129–193)

Gage, J. D. (1996). Why are there so many species in deep-sea sediments? Journal of Experimental Marine Biology and Ecology, 200(1–2), 257–286. DOI: 10.1016/S0022-0981(96)02638-X

Gage, J. D., and Tyler, P. A. (1991). Deep-sea biology: a natural history of organisms at the deep-sea floor. Cambridge University Press.

Gooday, A. J., Malzone, M. G., Bett, B. J., and Lamont, P. A. (2010). Decadal-scale changes in shallow-infaunal foraminiferal assemblages at the Porcupine Abyssal Plain, NE Atlantic. Deep Sea Research Part II: Topical Studies in Oceanography, 57(15), 1362-1382. DOI: 10.1016/j.dsr2.2010.01.012

Gooday, AJ., Bett, B.J. and Pratt, D.N. (1993). Direct observation of episodic growth in an abyssal xenophyophore (Protista). Deep Sea Research Part I: Oceanographic Research Papers. 40, 2131-2143. DOI: 10.1016/0967-0637(93)90094-J

Harris, P. T., Macmillan-Lawler, M., Rupp, J., and Baker, E. K. (2014). Geomorphology of the oceans. Marine Geology, 352, 4–24. DOI: 10.1016/j.margeo.2014.01.011

Hensen, C., Adao, H., Arn, S., Batista, L., Belosa, L., Bodenbinder, A., Cherednichenko, S., Domeyer, Bettina, Duarte, J., Glombitza, C., Kaul, N., Koppe, M., Li, J., Liebetrau, Volker, Müller, Thomas , Nogueira, P., Nuzzo, Marianne, Petersen, Asmus, Schmidt, Mark , Schmidt, J. N., Schmidt, T., Sroczynska, K., Stelzner, M., Terrinha, P., Warnken, N. and Weber, U. W. (2020). Exploring subsurface fluid flow and active dewatering along the oceanic plate boundary between Africa and Eurasia (Gloria Fault). DOI: 10.48433/cr_m162.

Hensen, C., Duarte, J., Vannucchi, P., Mazzini, A., Lever, M. A., Terrinha, P., Géli, L., Henry, P., Villinger, H., Morgan, J., Schmidt, M., Gutscher, M. A., Bartolome, R., Tomonaga, Y., Polonia, A., Gràcia, E., Tinivella, U., Lupi, M., Çağatay, M. N., et al. (2019). Marine transform faults and Fracture Zones: A joint perspective integrating seismicity, fluid flow and life. Frontiers in Earth Science, 7, 1–29. DOI: 10.3389/feart.2019.00039

Hensen, C., Nuzzo, M., Hornibrook, E., Pinheiro, L. M., Bock, B., Magalhães, V. H., and Brückmann, W. (2007). Sources of mud volcano fluids in the Gulf of Cadiz—indications for hydrothermal imprint. Geochimica et Cosmochimica Acta, 71(5), 1232-1248. DOI: 10.1016/j.gca.2006.11.022

Hensen, C., Scholz, F., Nuzzo, M., Valadares, V., Gràcia, E., Terrinha, P., Liebetrau, V., Kaul, N., Silva, S., Martinez-Loriente, S., Bartolome, R., Pinero, E., Magalhães, V. H., Schmidt, M., Weise, S. M., Cunha, M., Hilario, A., Perea, H., Rovelli, L., and Lackschewitz, K. (2015). Strike-slip faults mediate the rise of crustal-derived fluids and mud volcanism in the deep sea. Geology, 43(4), 339-342. DOI: 10.1130/G36359.1

Howell, K. L., Hilário, A., Allcock, A. L., Bailey, D. M., Baker, M., Clark, M. R., Colaço, A., Copley, J., Cordes, E. E., Danovaro, R., Dissanayake, A., Escobar, E., Esquete, P., Gallagher, A. J., Gates, A. R., Gaudron, S. M., German, C. R., Gjerde, K. M., Higgs, N. D., et al. (2020a). A Blueprint for an Inclusive, Global Deep-Sea Ocean Decade Field Program. Frontiers in Marine Science, 7, 1–25. DOI: 10.3389/fmars.2020.584861

Howell, K. L., Hilário, A., Allcock, A. L., Bailey, D., Baker, M., Clark, M. R., Colaço, A., Copley, J., Cordes, E. E., Danovaro, R., Dissanayake, A., Escobar, E., Esquete, P., Gallagher, A. J., Gates, A. R., Gaudron, S. M., German, C. R., Gjerde, K. M., Higgs, N. D., et al. (2020b). A decade to study deep-sea life. Nature Ecology and Evolution, 5, 265–267. DOI: 10.1038/s41559-020-01352-5

Howell, K.L., Davies J.S. and van den Beld I. (2017) Deep-sea species image catalogue. University of Plymouth, Ifremer, NOAA. From http://www.deepseacatalogue.fr

Kalogeropoulou, V., Bett, B. J., Gooday, A. J., Lampadariou, N., Arbizu, P. M., and Vanreusel, A. (2010). Temporal changes (1989–1999) in deep-sea metazoan meiofaunal assemblages on the Porcupine Abyssal Plain, NE Atlantic. Deep Sea Research Part II: Topical Studies in Oceanography, 57(15), 1383-1395. DOI: 10.1016/j.dsr2.2009.02.002

Kuhnz, L. A., Ruhl, H. A., Huffard, C. L., and Smith, K. L. (2020). Benthic megafauna assemblage change over three decades in the abyss: Variations from species to functional groups. Deep Sea Research Part II: Topical Studies in Oceanography, 173, 104761. DOI: 10.1016/j.dsr2.2020.104761

Kutti, T., Bannister, R. J., and Fosså, J. H. (2013). Community structure and ecological function of deep-water sponge grounds in the Traenadypet MPA—Northern Norwegian continental shelf. Continental Shelf Research, 69, 21-30. DOI: 10.1016/j.csr.2013.09.011

Lampitt, R.S. and Paterson, G.L.J. (1987). The feeding behaviour of an abyssal sea anemone from in situ time lapse photographs and trawl samples. Oceanologica Acta, 10, 445-461.

Lavelle, J. W., and Mohn, C. (2010). Motion, commotion, and biophysical connections at deep ocean seamounts. Oceanography, 23(1), 90-103. DOI: 10.5670/oceanog.2010.64

Levin, L. A. (1991). Interactions between metazoans and large, agglutinating protozoans: implications for the community structure of deep-sea benthos. American Zoologist, 31(6), 886-900. DOI: 10.1093/icb/31.6.886

Levin, L. A., Etter, R. J., Rex, M. A., Gooday, A. J., Smith, C. R., Pineda, J., Stuart, C. T., Hessler, R. R., and Pawson, D. (2001). Environmental influences on regional deep-sea species diversity. Annual Review of Ecology and Systematics, 32, 51–93. DOI: 10.1146/annurev.ecolsys.32.081501.114002

Liu, M., and Tanhua, T. (2021). Water masses in the Atlantic Ocean: Characteristics and distributions. Ocean Science, 17(2), 463–486. DOI: 10.5194/os-17-463-2021

Lonsdale, P. (1977). Clustering of suspension-feeding macrobenthos near abyssal hydrothermal vents at oceanic spreading centers. Deep Sea Research, 24(9), 857-863. DOI: 10.1016/0146-6291(77)90478-7

Lutz, M. J., Caldeira, K., Dunbar, R. B., and Behrenfeld, M. J. (2007). Seasonal rhythms of net primary production and particulate organic carbon flux to depth describe the efficiency of biological pump in the global ocean. Journal of Geophysical Research: Oceans, 112(C10). DOI: 10.1029/2006JC003706

MacDonald, I. R., Bluhm, B. A., Iken, K., Gagaev, S., and Strong, S. (2010). Benthic macrofauna and megafauna assemblages in the Arctic deep-sea Canada Basin. Deep Sea Research Part II: Topical Studies in Oceanography, 57(1-2), 136-152. DOI: 10.1016/j.dsr2.2009.08.012

Maldonado, M., Aguilar, R., Bannister, R., Bell, J., Conway, K., Dayton, P. (2015) Sponge grounds as key marine habitats: a synthetic review of types, structure, functional roles and conservation concerns. In: S. Rossi, L. Bramanti, A. Gori, C. Orejas Saco del Valle (Eds.), Marine Animal Forests: The Ecology of Benthic Biodiversity Hotspots. (pp. 145–183). Springer. DOI: 10.1007/978-3-319-17001-5_24-1

Marcon, Y., and Purser, A. (2017). PAPARA (ZZ) I: An open-source software interface for annotating photographs of the deep-sea. SoftwareX, 6, 69-80.

Marine Species Traits editorial board (2021). Marine Species Traits. http://www.marinespecies.org/traits (Acessed 10 November 2021)

Martinez, E., Antoine, D., D'Ortenzio, F., and De Boyer Montégut, C. (2011). Phytoplankton spring and fall blooms in the North Atlantic in the 1980s and 2000s. Journal of Geophysical Research: Oceans, 116(11), 1–11. DOI: 10.1029/2010JC006836

Meysman, F. J., Middelburg, J. J., and Heip, C. H. (2006). Bioturbation: a fresh look at Darwin's last idea. Trends in Ecology and Evolution, 21(12), 688-695. DOI: 10.1016/j.tree.2006.08.002

Molodtsova, T. N., Sanamyan, N. P., and Keller, N. B. (2008). Anthozoa from the northern Mid-Atlantic Ridge and Charlie-Gibbs Fracture Zone. Marine Biology Research, 4(1-2), 112-130. DOI: 10.1080/17451000701821744

Morris, K. J., Bett, B. J., Durden, J. M., Benoist, N. M., Huvenne, V. A., Jones, D. O., Robert, K., Ichino, M. C., Wolff, G. A. and Ruhl, H. A. (2016). Landscape-scale spatial heterogeneity in phytodetrital cover and megafauna biomass in the abyss links to modest topographic variation. Scientific reports, 6(1), 1-10. DOI: 10.1038/srep34080

NOAA Ocean Exploration. (2021). Benthic Deepwater Animal Identification Guide V3. http://oceanexplorer.noaa.gov/okeanos/animal_guide/animal_guide.html. (Accessed 10 April 2021)

Nunnally, C. C., Benfield, M. C., and McClain, C. R. (2020). Trait-based diversity of deep-sea benthic megafauna communities near the Deepwater Horizon oil spill site. Marine Ecology, 41(5), e12611. DOI: 10.1111/maec.12611

Oliveira, F., Aguilar, R., Monteiro, P., Bentes, L., Afonso, C.M.L., Garcia, S., Xavier, J.R., Ocañia, O., de Malos, V., Tavares, A.M., Gonçalves, J.M.S. (2017). A photographic guide of the species of the Gorringe Bank. Centro de Ciências do Mar (CCMARI/Oceana).

Omira, R., Neres, M., and Batista, L. (2019). The Gloria transform fault—NE Atlantic: seismogenic and tsunamigenic potential. In: J. C. Duarte (Ed), Transform Plate Boundaries and Fracture Zones (pp. 157-167) Elsevier. DOI: 10.1016/B978-0-12-812064-4.00008-6

Pape, E., Bezerra, T. N., Gheerardyn, H., Buydens, M., Kieswetter, A., and Vanreusel, A. (2021). Potential impacts of polymetallic nodule removal on deep-sea meiofauna. Scientific reports, 11(1), 1-15.

Pham, C. K., Ramirez-Llodra, E., Alt, C. H. S., Amaro, T., Bergmann, M., Canals, M., Company, J. B., Davies, J., Duineveld, G., Galgani, F., Howell, K. L., Huvenne, V. A. I., Isidro, E., Jones, D. O. B., Lastras, G., Morato, T., Gomes-Pereira, J. N., Purser, A., Stewart, H., et al. (2014). Marine litter distribution and density in European seas, from the shelves to deep basins. PLoS ONE, 9(4). DOI: 10.1371/journal.pone.0095839

Puerta, P., Johnson, C., Carreiro-Silva, M., Henry, L. A., Kenchington, E., Morato, T., Kazadinis, G., Rueda, J. L., Urra, J., Ross, S., Wei, C. L., González-Irusta, J. M., Arnaud-Haond, S. and Orejas, C. (2020). Influence of water masses on the biodiversity and biogeography of deep-sea benthic ecosystems in the North Atlantic. Frontiers in Marine Science, 7, 239. DOI: 10.3389/fmars.2020.00239

Ramirez-Llodra, E., Brandt, A., Danovaro, R., De Mol, B., Escobar, E., German, C. R., Levin, L. A., Martinez Arbizu, P., Menot, L., Buhl-Mortensen, P., Narayanaswamy, B. E., Smith, C. R., Tittensor, D. P., Tyler, P. A., Vanreusel, A., and Vecchione, M. (2010). Deep, diverse and definitely different: Unique attributes of the world's largest ecosystem. Biogeosciences, 7(9), 2851–2899. DOI: 10.5194/bg-7-2851-2010

Ramirez-Llodra, E., Tyler, P. A., Baker, M. C., Bergstad, O. A., Clark, M. R., Escobar, E., Levin, L. A., Menot, L., Rowden, A. A., Smith, C. R., and van Dover, C. L. (2011). Man and the last great wilderness: Human impact on the deep sea. PLoS ONE, 6(8). DOI: 10.1371/journal.pone.0022588

Rex, M. A. (1981). Community Structure in the Deep-Sea Benthos. Annual Review of Ecology and Systematics, 12(1), 331–353. DOI:10.1146/annurev.es.12.110181

Rex, M. A., Etter, R. J., Morris, J. S., Crouse, J., McClain, C. R., Johnson, N. A., Stuart, C. T., Deming, J. W., Thies, R., and Avery, R. (2006). Global bathymetric patterns of standing stock and body size in the deep-sea benthos. Marine Ecology Progress Series, 317, 1–8. DOI: 10.3354/meps317001

Riehl, T., Wölfl, A. C., Augustin, N., Devey, C. W., and Brandt, A. (2020). Discovery of widely available abyssal rock patches reveals overlooked tiering type and prompts rethinking deep-sea biodiversity. Proceedings of the National Academy of Sciences of the United States of America, 117(27), 15450–15459. DOI: 10.1073/pnas.1920706117

Riemann-Zuerneck, K. (1997). A hemisessile sea anemone from the Porcupine Abyssal Plain, North Atlantic Ocean*: Iosactis vagabunda* gen. nov., sp. nov. Journal of the Marine Biological Association of UK. 77, 1011-1025. DOI: 10.1017/S0025315400038595

Ruhl, H. A., and Smith, K. L. (2004). Shifts in deep-sea community structure linked to climate and food supply. Science, 305(5683), 513–515. DOI: 10.1126/science.1099759

Schmidt, C., Hensen, C., Wallmann, K., Liebetrau, V., Tatzel, M., Schurr, S. L., Kutterolf, S., Haffert, L., Geilert, S., Hübscher, C., Lebas, E., Heuser, A., Schmidt, M., Strauss, H., Vogl, J., and Hansteen, T. (2019). Origin of High Mg and SO4 Fluids in Sediments of the Terceira Rift, Azores-Indications for Caminite Dissolution in a Waning Hydrothermal System. Geochemistry, Geophysics, Geosystems, 20(12), 6078–6094. DOI: 0.1029/2019GC008525

Seabed 2030. (2021). Mapping process. https://seabed2030.org/mapping-progress (Acessed 24 November 2021)

Serra, N., and Ambar, I. (2002). Eddy generation in the Mediterranean undercurrent. Deep Sea Research Part II: Topical Studies in Oceanography, 49(19), 4225-4243. DOI: 10.1016/S0967-0645(02)00152-2

Sibuet, M. (1985). Quantitative distribution of echinoderms (Holothuroidea, Asteroidea, Ophiuroidea, Echinoidea) in relation to organic matter in the sediment in deep basins of the Atlantic Ocean In B.F. Keegan and B.D.S. O'Connor (Eds.), Echinodermata (pp. 99–108). Balkema Rotterdam

Simon-Lledó, E., Bett, B. J., Huvenne, V. A. I., Schoening, T., Benoist, N. M. A., Jeffreys, R. M., Durden, J. M., and Jones, D. O. B. (2019). Megafaunal variation in the abyssal landscape of the Clarion Clipperton Zone. Progress in Oceanography, 170, 119–133. DOI: 10.1016/j.pocean.2018.11.003

Smith, C. R., and Baco, A. R. (2003). Ecology of Whale Falls at The Deep-Sea Floor. In Gibson, R. N. and Atkinson, R. J. A. (Eds.), Oceanography and Marine Biology: An Annual Review (pp. 612–613). Taylor and Francis.

Smith, C. R., De Leo, F. C., Bernardino, A. F., Sweetman, A. K., and Arbizu, P. M. (2008). Abyssal food limitation, ecosystem structure and climate change. Trends in Ecology and Evolution, 23(9), 518–528. DOI: 10.1016/j.tree.2008.05.002

Smith, C. R., Drazen, J., Mincks, S. L. (2006) Deep-sea Biodiversity and Biogeography: Perspectives from the Abyss. International Seabed Authority Seamount Biodiversity Symposium 2006.

Soto, E. H., Paterson, G. L., Billett, D. S., Hawkins, L. E., Galéron, J., and Sibuet, M. (2010). Temporal variability in polychaete assemblages of the abyssal NE Atlantic Ocean. Deep Sea Research Part II: Topical Studies in Oceanography, 57(15), 1396-1405. DOI: 10.1016/j.dsr2.2009.02.003

Strong, J. A., andonegi, E., Bizsel, K. C., Danovaro, R., Elliott, M., Franco, A., Garces, E., Little, L., Mazik, K., Moncheva, S., Porcupine Abyssal Plainadoupoulou, N., Patrício, J., Queirós, A. M., Smith, C., Stefanova, K. and Solaun, O. (2015). Marine biodiversity and ecosystem function relationships: the potential for practical monitoring applications. Estuarine, Coastal and Shelf Science, 161, 46-64. DOI: 10.1016/j.ecss.2015.04.008

Stuart, C. T., and Rex, M. A. (2009). Bathymetric patterns of deep-sea gastropod species diversity in 10 basins of the Atlantic Ocean and Norwegian Sea. Marine Ecology, 30(2), 164–180. DOI: 10.1111/j.1439-0485.2008.00269.x

Thurber, A. R., Sweetman, A. K., Narayanaswamy, B. E., Jones, D. O., Ingels, J., and Hansman, R. L. (2014). Ecosystem function and services provided by the deep sea. Biogeosciences, 11(14), 3941-3963. DOI: 10.5194/bg-11-3941-2014

Thurston, M. H., Bett, B. J., Rice, A. L., and Jackson, P. A. B. (1994). Variations in the invertebrate abyssal megafauna in the North Atlantic Ocean. Deep Sea Research Part I: Oceanographic Research Porcupine Abyssal Plainers, 41(9), 1321-1348. DOI: 10.1016/0967- 0637(94)90100-7

Thurston, M. H., Rice, A. L., and Bett, B. J. (1998). Latitudinal variation in invertebrate megafaunal abundance and biomass in the North Atlantic Ocean Abyss. Deep Sea Research Part II: Topical Studies in Oceanography, 45(1-3), 203-224. DOI: 10.1016/S0967-0645(97)00077-5

Tyler, P. A. (2003). Ecosystems of the deep oceans. Elsevier.

Vanreusel, A., Fonseca, G., Danovaro, R., Da Silva, M. C., Esteves, A. M., Ferrero, T., Gad, G., Galtsova, V., Gambi, C., Genevois, V. F., Ingels, J., Ingole, B., Lampadarious, N., Merckx, B., Miljutin, D., Mijutina, M. Muthumbi, A., Netto, S., et al. (2010). The contribution of deep-sea macrohabitat heterogeneity to global nematode diversity. Marine Ecology, 31(1), 6-20. DOI: 10.1111/j.1439-0485.2009.00352.x

Vanreusel, A., Hilario, A., Ribeiro, P. A., Menot, L., and Arbizu, P. M. (2016). Threatened by mining, polymetallic nodules are required to preserve abyssal epifauna. Scientific reports, 6, Article number 26808. DOI: 10.1038/srep26808

Vieira, R. P., Raposo, I. P., Sobral, P., Gonçalves, J. M., Bell, K. L., and Cunha, M. R. (2015). Lost fishing gear and litter at Gorringe Bank (NE Atlantic). Journal of sea research, 100, 91-98. DOI: 10.1016/j.seares.2014.10.005

Wagner, H. H., Wildi, O., Ewald, K. C. (2000). Additive partitioning of plant species diversity in an agricultural mosaic landscape. Landscape Ecology 15:219–227. DOI: 10.1023/A:1008114117913

Ziegler, A. F., Smith, C. R., Edwards, K. F., and Vernet, M. (2017). Glacial dropstones: islands enhancing seafloor species richness of benthic megafauna in West Antarctic Peninsula fjords. Marine Ecology Progress Series, 583, 1-14. DOI: 10.3354/meps12363

ANNEX

Table A1 - PERMDISP pair-wise comparisons between work areas based on the measured environmental. Values in bold correspond to significant values.

Pairwise comparisons		
Groups	**t**	**P(perm)**
WA01, WA02	9.9447	**0.0001**
WA01, WA04	6.1841	**0.0001**
WA01, WA06	0.96682	0.5085
WA02, WA04	2.0087	0.0795
WA02, WA06	1.9468	0.18
WA04, WA06	0.8771	0.6941

Table A2 - PERMANOVA main test results based on the measured environmental variables. Values in bold correspond to significant values.

Source	df	SS	MS	Pseudo-F	P(perm)	Perm
Work area	3	1847.6	615.87	80.003	**0.0035**	4339
Station (Work area)	3	3.5459	1.182	12.928	**0.0008**	9918
Res	228	20.845	0.091427			
Total	234	1872				

Table A3 - PERMANOVA pair-wise comparisons between work areas based on environmental variables. Values in bold correspond to significant values. When the permutations number was low, Monte Carlo p-value (P(MC)) was considered.

Pairwise comparisons				
Groups	**t**	**P(perm)**	**Perm**	**P (MC)**
WA01, WA02	10.101	0.1648	24	**0.0045**
WA01, WA04	12.885	0.1662	6	**0.0205**
WA01, WA06	112.21	**0.0001**	9877	0.0001
WA02, WA04	2.0627	0.1311	120	0.062
WA02, WA06	7.4182	0.1703	24	**0.0046**
WA04, WA06	9.7038	0.0001	6	**0.0143**

Table A4 –PERMDISP pairwise comparisons based on total mega-epifaunal and *lebensspuren* densities registered for all replicates Values in bold correspond to significant values.

Total mega-epifauna density		
Groups	**t**	**P(perm)**
WA01, WA02	18.452	**0.0001**
WA01, WA04	8.2563	**0.0001**
WA01, WA06	9.8734	**0.0001**
WA02, WA04	6.1645	0.0014
WA02, WA06	31.235	**0.0001**
WA04, WA06	16.125	**0.0001**

Total *lebensspuren* density		
Groups	**t**	**P(perm)**
WA01, WA02	5.6477	**0.0001**
WA01, WA04	9.5553	**0.0001**
WA01, WA06	16.506	**0.0001**
WA02, WA04	8.4433	**0.0001**
WA02, WA06	16.753	**0.0001**
WA04, WA06	4.24	**0.0026**

Table A5 - PERMANOVA main test results based on total mega-epifaunal and *lebensspuren* density . Values in bold correspond to significant values.

Source	Total mega-epifauna density					
	df	**SS**	**MS**	**Pseudo-F**	**P(perm)**	**Perm**
Work area	3	154.53	51.509	71.449	**0.026**	4345
Station (Work area)	3	1.716	0.572	1.0206	0.3794	9950
Res	1781	998.14	0.56044			
Total	1781	1154.4				

Source	Total *lebensspuren* density					
	df	**SS**	**MS**	**Pseudo-F**	**P(perm)**	**Perm**
Work area	**3**	3771.8	1257.3	2.5511	0.2731	4357
Station (Work area)	**3**	1171.7	390.56	47.994	**0.0001**	9958
Res	1781	14493	8.1378			
Total	1781	19437				

Table A6 - PERMANOVA pairwise comparisons based on total mega-epifaunal and *lebensspuren* densities. Values in bold correspond to significant values. When the permutations number was low, Monte Carlo p-values (P(MC)) was considered.

Groups	Total mega-epifauna density Pairwise comparisons			
	t	**P(perm)**	**Perm**	**P (MC)**
WA01, WA02	31.151	0.0843	24	**0.0008**
WA01, WA04	1.9672	0.0001	6	0.3056
WA01, WA06	5.3722	**0.0001**	9822	0.0001
WA02, WA04	1.0419	0.2995	120	0.3751
WA02, WA06	75.539	0.1272	24	**0.0003**
WA04, WA06	5.2166	0.0001	6	0.1181

Groups	Total *lebensspuren* density Pairwise comparisons			
	t	**P(perm)**	**Perm**	**P (MC)**
WA01, WA02	1.0022	0.2479	24	0.4348
WA01, WA04	0.43348	0.6675	6	0.7475
WA01, WA06	16.462	**0.0001**	9843	0.0001
WA02, WA04	1.0387	0.2975	120	0.3695
WA02, WA06	11.111	0.167	24	**0.0085**
WA04, WA06	0.67134	0.5041	6	0.6298

Table A7 - PERMDISP pair-wise comparisons between work areas based on composition. Values in bold correspond to significant values.

Pairwise comparisons		
Groups	**t**	**P(perm)**
WA01, WA02	1.397	0.2431
WA01, WA04	1.9269	0.127
WA01, WA06	7.8805	**0.0001**
WA02, WA04	2.6558	**0.0176**
WA02, WA06	4.6042	**0.0027**
WA04, WA06	2.1265	0.1421

Table A8 - PERMANOVA main test results based on composition. Values in bold correspond to significant values.

Source	df	SS	MS	Pseudo-F	P(perm)	Perm
Work area	3	2.44E+05	81467	1.2506	0.3037	4312
Station (Work area)	3	36545	12182	3.7688	**0.0001**	9881
Res	228	7.37E+05	3232.2			
Total	234	1.02E+06				

Table A9 - Results of the distance based linear model (DISTLM) analysis for investigating the relationship between mega-epifauna and environmental variables. Marginal tests: variation for each variable alone. Sequential tests: conditional testing of variables for the best model based on the selection criterion of adjusted R~2.

Marginal tests			
Variable	**Pseudo-F**	**P**	**Prop.**
Depth	10.471	0.0001	0.043006
Salinity	25.054	0.0001	0.097087
Temperature	32.749	0.0001	0.12323
Turbidity	52.328	0.0001	0.1834
Oxygen	27.354	0.0001	0.10507
Methane	50.027	0.0001	0.17676
NPP	43.137	0.0001	0.15622
SVI	43.522	0.0001	0.15739

Sequential tests					
Variable	**Adj R^2**	**Pseudo-F**	**P**	**Prop.**	**Cumul.**
Turbidity	0.17989	52.328	0.0001	0.1834	0.1834
Salinity	0.22221	13.678	0.0001	0.045464	0.22886
SVI	0.24062	6.6221	0.0001	0.02149	0.25035
Depth	0.2512	4.2664	0.0002	0.013652	0.264
NPP	0.25744	2.9311	0.0037	0.009301	0.27331
Oxygen	0.26085	2.0582	0.0374	0.006501	0.27981
Temperature	0.26402	1.9795	0.0662	0.006226	0.28603
Methane	0.26416	1.0458	0.376	0.003289	0.28932

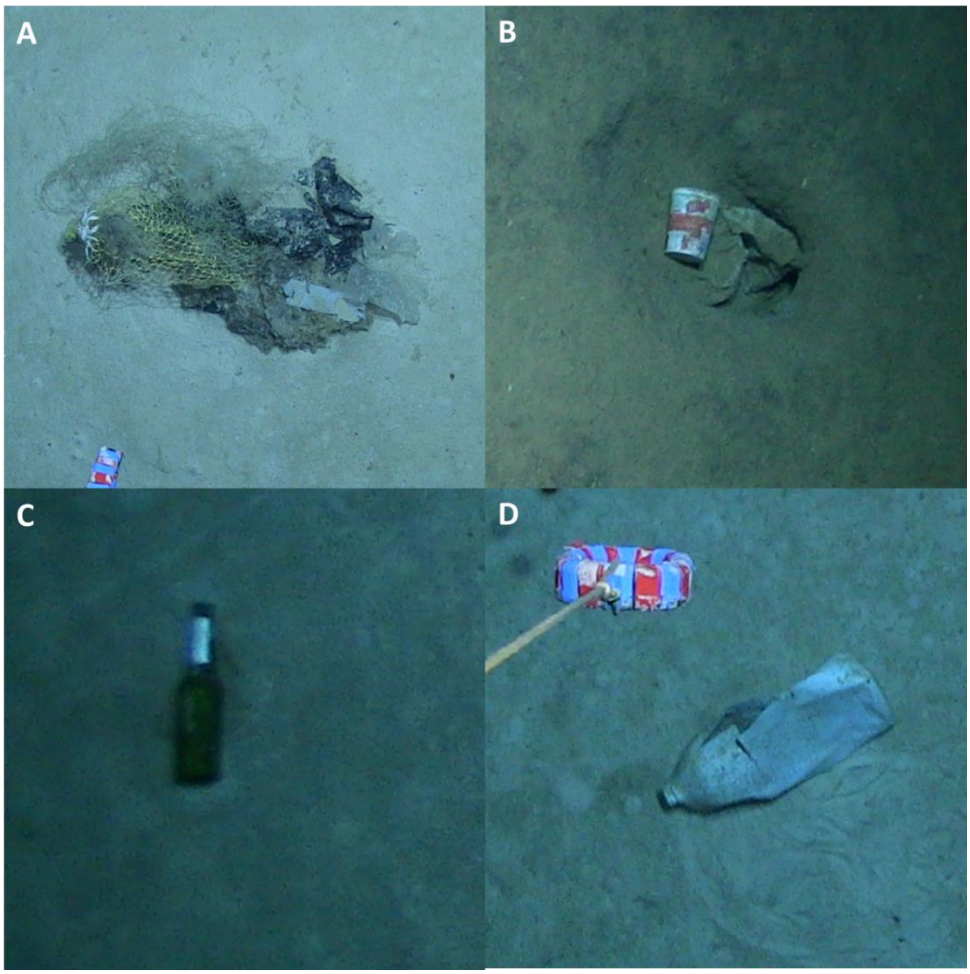

Figure 1A – Examples of different types of marine litter observed across the Gloria Fault, including **(A)** fishing gear with a Galatheidae, **(B)** a plastic/yougurt cup, **(C)** a glass bottle and **(D)** a plastic container**.**